

# NASA TECHNICAL MEMORANDUM

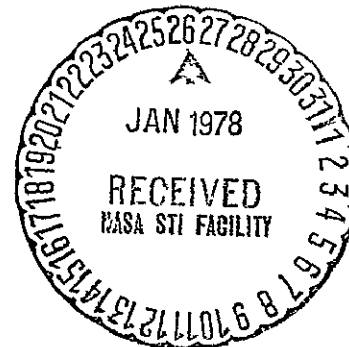
NASA TM-73820

NASA TM-73820

(NASA-TM-73820) TECHNICAL AND ECONOMIC FEASIBILITY STUDY OF SOLAR/FOSSIL HYBRID POWER SYSTEMS (NASA) 70 p HC A04/MF A01	N78-17486
CSCI 10B	Unclas 57797
	G3/44

## TECHNICAL AND ECONOMIC FEASIBILITY STUDY OF SOLAR/FOSSIL HYBRID POWER SYSTEMS

by Harvey S. Bloomfield and James E. Calogeras  
 Lewis Research Center  
 Cleveland, Ohio 44135  
 December 1977



1. Report No NASA TM-73820	2. Government Accession No.	3. Recipient's Catalog No.	
4. Title and Subtitle <b>TECHNICAL AND ECONOMIC FEASIBILITY STUDY OF SOLAR/FOSSIL HYBRID POWER SYSTEMS</b>		5. Report Date December 1977	6. Performing Organization Code
		8. Performing Organization Report No E-9409	10. Work Unit No.
7. Author(s) Harvey S. Bloomfield and James E. Calogeras		11. Contract or Grant No.	
9. Performing Organization Name and Address National Aeronautics and Space Administration Lewis Research Center Cleveland, Ohio 44135		13. Type of Report and Period Covered Technical Memorandum	
		14. Sponsoring Agency Code	
12. Sponsoring Agency Name and Address National Aeronautics and Space Administration Washington, D.C. 20546		15. Supplementary Notes	
16. Abstract A preliminary feasibility study of solar/fossil hybrid power systems was conducted to evaluate the overall economic and technical aspects of this class of solar electric power system. Results show that new hybrid systems utilizing fossil fuel augmentation of solar energy can provide significant capital and energy cost benefits when compared with solar thermal systems requiring thermal storage. These benefits accrue from a reduction of solar collection area that results from both the use of highly efficient gas and combined cycle energy conversion subsystems and elimination of the requirement for long-term energy storage subsystems. Technical feasibility and fuel savings benefits of solar hybrid retrofit to existing fossil-fired, gas and vapor cycle powerplants was confirmed; however, economic viability of steam cycle retrofit was found to be dependent on the thermodynamic and operational characteristics of the existing powerplant.			
17. Key Words (Suggested by Author(s)) Solar energy conversion Electric powerplants Solar/fossil hybrid systems		18. Distribution Statement Unclassified - unlimited STAR Category 44	
19. Security Classif (of this report) Unclassified	20. Security Classif (of this page) Unclassified	21. No. of Pages	22. Price*

## INTRODUCTION

A national program to demonstrate the achievement of large-scale conversion of solar energy to electricity is currently underway. A major goal of this program is to develop and demonstrate the technology required to establish technical feasibility and indicate economic viability of solar electric power systems.

In considering the integration of solar thermal conversion powerplants into an electrical power grid the issues of capacity and energy displacement must be assessed. The capability of solar powerplants to displace conventional generating capacity will be impacted by outages due to reduced solar radiation because of cloud cover or during nonsunlight hours. In addition, this impact will vary for different operating modes such as baseload, intermediate, or peaking. The effect of solar insolation outage can be reduced or compensated for by providing an energy storage subsystem to maintain a continuity of useful output. Although no systems suitable for large-scale energy storage have yet been fabricated; several organizations are conducting studies to integrate thermal energy storage (TES) subsystems with solar powerplants. At least three organizations are currently developing prototype TES systems for solar thermal applications.

An alternate concept to compensate for solar insolation outage is to combine solar and fossil-fueled subsystems in a common powerplant. This is referred to as a hybrid solar thermal system. For the study reported herein, hybrid solar thermal systems are defined to utilize both solar and fossil fuel energy to provide thermal input to an energy conversion subsystem in a single-site powerplant. Hybrid systems are applicable to existing conventional powerplants (retrofit) or to new or advanced powerplant concepts. The energy conversion subsystem used in a hybrid system may operate on any thermodynamic power cycle. The fossil fuel used may be gas, oil, coal or coal-derived synthetic. The solar energy collection subsystem may be flat plate, parabolic trough or dish, heliostat/tower, or any combination of these. In addition, the solar and fossil fuel energy may be combined in either of two operational modes. In the first mode, the energy conversion subsystem operates solely on solar energy during periods of high solar insolation and fossil fuel is used as "storage" - only to be used during periods of solar outage. This type of

operation appears suitable for applications where the temperature levels available from current solar collection subsystems are sufficient to heat a working fluid to attractive energy conversion cycle peak temperatures. The second, and potentially more versatile, mode of hybrid system operation utilizes fossil fuel energy to augment the solar energy source to provide a temperature increase of the energy conversion cycle working fluid. This mode can still provide a "storage" capability as in the first mode, for operation during periods of solar outage. The augment type of hybrid system operation enables the potential use of the high temperature, high efficiency, energy conversion systems currently available with gas turbines and combined cycles.

It is obvious that the hybrid system concept may be employed in a wide variety of potentially attractive solar thermal systems. The object of this report is to investigate the relative merits of each system in sufficient detail to permit an assessment of technical and economic viability.

This report concludes a study initiated by the NASA Lewis Research Center at the request of the Solar Energy Division of the Energy Research and Development Administration (ERDA) in February 1976. The study was conducted by a Task Team (Appendix A) from the NASA Lewis, Power Generation and Storage Division. The Task Team obtained recommendations, support, and advice from a variety of sources. Inputs were solicited from a NASA-Lewis Advisory Panel (Appendix B), from major prime mover manufacturers, from utilities and architect-engineering firms, and from other government and nonprofit agencies and organizations. A list of the outside source contacts utilized is shown in appendix C. The Task Team developed the final study recommendations reflecting counsel received from the advisors and source contacts.

## STUDY DEFINITION

### Goal

The goal of this study was to provide a preliminary assessment of the technical feasibility and economic viability of retrofit, new, and advanced hybrid solar thermal electric power system concepts.

## Objectives

The overall objectives of this study were to provide a basis for technical and economic comparison of hybrid system concepts with other solar thermal electric generation systems and conventional powerplants, and to conduct a preliminary assessment of attractive concepts.

The specific objectives included:

1. Identification of candidate hybrid energy conversion subsystems in terms of technical feasibility, efficiency, and fuel savings.
2. Establishment of the functional and operational aspects, and technology development requirements of a variety of retrofit, new and advanced hybrid system concepts.
3. Parametric economic sensitivity assessment of a range of hybrid systems including cost of electricity comparisons with solar thermal systems utilizing energy storage, and conventional powerplants.

## General Approach

The approach taken to achieve the study objectives was to perform parallel technical and economic analyses of hybrid solar thermal systems. Initial identification of a matrix of candidate hybrid system concepts was the first task of the Technical Analysis phase. Reference design concepts and ranges of operational parameters were established. Parametric analyses of selected available energy conversion subsystems (table I) were conducted with respect to performance and fuel savings characteristics. Assessment of engineering constraints and technology development requirements were carried out for the selected energy conversion design configurations. These assessments were obtained from a variety of sources including a NASA-Lewis advisory panel, the utility industry, architect-engineering firms, and manufacturers and vendors of prime movers and associated equipment.

The economic analysis phase of the study began with the establishment of an assessment methodology designed to allow system comparisons on a normalized and consistent basis. The operational characteristics of each system were then selected to provide known solar and fossil fuel duration times.

Capital cost estimates for solar; storage, hybrid; and energy conversion subsystems were based on current technology for the required components. Parametric analyses of all systems over a range of expected capital costs were performed and cost of electricity comparisons were made including comparisons with specific conventional all-fossil systems.

A flow diagram of the study methodology is presented in figure 1.

## RESULTS AND DISCUSSION

### Technical Analysis

The details of the methodology used to arrive at the results presented in this section are given in appendix D. The results of the technical analysis effort that follows are divided into the following subsections: (a) Simple and Recuperated Open Gas Turbine Cycles; (b) Combined Cycles - 1. Unfired - 2 - Supplemental Firing; (c) Component and System Considerations; (d) Vapor Cycles.

#### (a) Simple and Recuperated Open Gas Turbine Cycles

Schematic diagrams of the simple and recuperated cycles considered in the parametric analyses are presented in figures 2 and 3. The numbering system corresponding to station locations is consistent throughout the analyses. Solar thermal energy input is shown in series with the fossil fuel energy input. This was the only configuration considered in the technical analysis from a calculational aspect. The justification and technical ramifications of this mode of operation (versus a parallel configuration) are discussed in a later subsection titled Component and System Considerations.

Thermal cycle efficiency is presented in figure 4 as a function of compressor pressure ratio for the simple open cycle gas turbine system. Each curve represents a constant peak cycle operating temperature (or turbine inlet temperature,  $T_5$ ). These results are based on a solar input temperature of  $982^{\circ}\text{C}$  ( $1800^{\circ}\text{F}$ ), and will show slight variations with different values. The range of solar input temperatures investigated was from  $427^{\circ}\text{C}$  ( $800^{\circ}\text{F}$ ) to  $1204^{\circ}\text{C}$  ( $2200^{\circ}\text{F}$ ). For the cases of solar input temperature less than turbine

inlet requirements sufficient amounts of fossil fuel were combusted to achieve the higher turbine inlet temperatures.

The results of figure 4 indicate maximum simple thermal cycle efficiencies occur at high compressor pressure ratios and vary from about 29-percent at a turbine inlet temperature of  $982^{\circ}\text{C}$  to about 34-percent at a turbine inlet temperature of  $1204^{\circ}\text{C}$ .

The effect of utilizing heat energy available from the turbine discharge in a recuperated cycle with an assumed effectiveness of 0.8 is presented in figure 5. Results correspond to the same turbine inlet temperatures and solar input temperature presented in the previous figure.

In this cycle, maximum thermal cycle efficiencies occur with lower compressor pressure ratios and vary from about 40 percent at a turbine inlet temperature of  $982^{\circ}\text{C}$  to 45 percent at a turbine inlet temperature of  $1204^{\circ}\text{C}$ . These efficiencies represent a major improvement over the simple cycle, or unrecuperated gas turbine system. However, simple cycle retrofit applications can provide significant fuel savings as will be discussed later in this section.

The maximum thermal cycle efficiencies computed over the range of turbine inlet temperatures and recuperator effectivenesses included in this study are presented in figure 6 as a function of optimum CPR for a solar heat input temperature of  $982^{\circ}\text{C}$  ( $1800^{\circ}\text{F}$ ). These curves represent systems in which the CPR has been selected to provide maximum system efficiency.

Optimum CPR varies from about 3:1 for a recuperated system with an effectiveness of 0.95 from 14:1 to 21:1 for an unrecuperated or simple cycle. Considerations of the impact of such a large range of possible CPR's on compressor design and performance are contained in the section, Component and System Considerations.

The previous discussions relating to cycle efficiency were based on a fixed value of solar energy input temperature. The range of solar energy input, or solar receiver outlet, temperatures investigated was  $482^{\circ}\text{C}$  ( $900^{\circ}\text{F}$ ) to  $1204^{\circ}\text{C}$  ( $2200^{\circ}\text{F}$ ), as mentioned previously.

The achievement of solar receiver outlet working fluid temperatures in excess of about  $760^{\circ}\text{C}$  ( $1400^{\circ}\text{F}$ ) will require technology advancement beyond the current state of the art for metallic tube heat exchangers using air as the

working fluid. This is due to the nonuniformity of solar flux within a simple cavity tube receiver which causes nonuniform temperatures around the tubes leading to circumferential thermal stresses which can result in unacceptable thermal fatigue life (ref. 3).

The effect of solar energy input temperature on fuel savings is shown in figures 7 and 8 for simple and recuperated ( $\epsilon = 0.8$ ) open cycle gas turbines, respectively, in terms of fuel energy saved per unit of electrical energy generated. The parameters shown are turbine inlet temperature and percent solar energy input to the hybrid plant. The computer results have been generated for optimum compressor pressure ratios and are therefore representative of efficiency optimized systems. The values of fuel savings shown in the figures represent only the solar energy contribution and do not include the additional savings that accrue from the increased efficiency of optimized CPR designs.

The potential fuel savings for a solar hybrid retrofit of an existing simple open cycle gas turbine powerplant can be obtained from figure 7. This type of combustion turbine powerplant is in widespread use by the utility industry to provide peaking service. Furthermore, nonelectrical generation versions of these turbines are also used extensively by the gas transmission industry for pumping service. Solar energy input to the air working fluid is assumed to be provided by a conventional metal tube heat exchanger (receiver) operating at an average temperature of  $760^{\circ}\text{C}$  ( $1400^{\circ}\text{F}$ ). For a typical turbine inlet temperature of  $982^{\circ}\text{C}$  ( $1800^{\circ}\text{F}$ ) and a solar input of about 60 percent, a fuel savings of 6500 Btu/kWe hr is obtained from figure 7. Assuming an average fuel cost of \$2.84/GJ (\$3.00/M Btu) over the remaining plant lifetime, and a 3000 hour annual solar duration and operating time, the annual solar fuel savings is approximately \$59/kWe. If half of the existing domestic electrical utility peaking gas turbine capacity (40 000 MWe) could be retrofit as described, and operated in the above mode, an equivalent of 80 million barrels of oil could be saved annually.



## b. Combined Cycles

### 1. Unfired

A schematic diagram of the combined cycle hybrid system considered in the parametric analysis is shown in figure 9. This system consists of an unfired steam Rankine cycle topped by an optionally recuperated open gas turbine cycle. Energy flows are distinguished from fluid flows for clarity and the numbering system corresponding to station locations is consistent with other cycles analyzed. Solar thermal energy input is shown in series with fossil fuel energy input. This was the only configuration considered in the technical analysis of combined cycles. The technical ramifications of this mode of operation (versus a parallel configuration) are discussed in a later subsection titled Component and System Considerations.

Maximum combined cycle thermal efficiencies were computed over a range of turbine inlet temperatures from  $982^{\circ}\text{C}$  ( $1800^{\circ}\text{F}$ ) to  $1204^{\circ}\text{C}$  ( $2200^{\circ}\text{F}$ ) and a gas turbine recuperator effectiveness from 0.0 (simple gas turbine cycle) to 0.8. The results are presented in figure 10. The CPR's shown correspond to maximum combined cycle efficiency, rather than maximum gas turbine cycle efficiency.

Over the range of parametric variations in this study, combined cycle thermal efficiency varied from about 44 percent for a simple gas turbine topping cycle to about 54 percent for a recuperated gas turbine cycle with  $\epsilon = 0.8$ . However, incorporation of significant recuperation (e.g.,  $\epsilon = 0.7, 0.8$ ) results in decreased steam temperatures. As discussed in appendix D this yields values of combined cycle efficiency that could be optimistic for steam temperatures below about  $371^{\circ}\text{C}$  ( $700^{\circ}\text{F}$ ).

Steam temperatures computed for various values of peak gas turbine cycle operating temperature,  $T_5$ , and recuperator effectiveness,  $\epsilon$ , are listed in table II. With a possible exception at  $T_5 = 1204^{\circ}\text{C}$  ( $2200^{\circ}\text{F}$ ), the steam temperatures corresponding to  $\epsilon = 0.7$  and  $\epsilon = 0.8$  dictate pressures below the  $12.4\text{ MN/m}^2$  (1800 psi) level assumed in this analysis. A more detailed study would have considered both saturation temperature and pressure, and the degree of superheat would have been adjusted to correspond to thermodynamic and operational practice.

Results previously presented in figures 6 and 10 are combined in figure 11 for comparison. Several interesting application aspects of gas turbine cycle selection can be shown by this figure.

For new hybrid gas turbine applications, figure 11 indicates potential performance trade-offs between combined cycle and recuperated cycle gas turbine powerplants. For example, a thermal cycle efficiency of 45 percent can be obtained with a nonrecuperated combined cycle operating at a peak cycle temperature of approximately 1900° F and a pressure ratio of about 11. The same efficiency is also obtainable with a recuperated cycle operating at a temperature of 1800° F, pressure ratio of about 4, and recuperator effectiveness near 0.9.

Both the recuperated and combined cycle plants considered are within the state-of-the-art. Therefore, cycle selection for new hybrid applications will depend more heavily on economic factors such as capital cost and cost of electricity.

For retrofit hybrid gas turbine applications a more detailed examination of cycle types and retrofit options is required. For example, hybrid retrofit to an existing fossil-fired, simple cycle gas turbine powerplant could be accomplished by the following changes in the energy conversion subsystem (in order of increasing cycle efficiency).

- (1) No change - (hybrid functions as fuel saver only)
- (2) Optimize pressure ratio for simple cycle
- (3) Add recuperator
- (4) Add recuperator and optimize pressure ratio
- (5) Add bottoming Rankine cycle
- (6) Add bottoming cycle and optimize pressure ratio
- (7) Add bottoming cycle and recuperator
- (8) Add bottoming cycle and recuperator and optimize pressure ratio

The benefits of each retrofit option must be analyzed from performance, cost, and engineering integration aspects for the particular cycle conditions of the existing powerplant.

The effect of variation of solar energy input temperature on fuel savings for an unrecuperated combined cycle is shown in figure 12. The parameters shown are gas turbine inlet temperature and hybrid solar energy percent. Solar energy input temperatures were calculated over the range  $482^{\circ}$  -  $983^{\circ}$  C ( $900^{\circ}$  -  $1800^{\circ}$  F), and values up to  $1204^{\circ}$  C ( $2200^{\circ}$  F) were extrapolated to provide estimates of fuel savings for 100 percent solar operation at all turbine inlet temperatures.

The values of fuel savings shown represent only the solar energy contribution and do not include the additional savings that accrue from the increased cycle efficiency of optimized CPR designs.

## 2. Supplemental Firing

A schematic diagram of a hybrid supplementally-fired combined cycle powerplant incorporating an optionally recuperated gas turbine cycle is shown in figure 13. The hybrid feature of this concept employs a straightforward arrangement of solar and fossil fuel input to the gas turbine cycle exhaust only. The concept does not utilize a high temperature solar receiver (heat exchanger) prior to the gas turbine inlet and, therefore, represents a lower temperature, near-term hybrid application. This application may be made to existing fossil-fueled supplementally-fired (nonrecuperated) combined cycles or as an add-on to an existing gas turbine plant. The add-on application could typically be taken by utilities wishing to upgrade peaking systems for longer operational times (ref. 2).

The hybrid supplemental firing concept was not included in the parametric technical analysis and, therefore, received only qualitative treatment.

Operational features of a conventional combined cycle incorporating supplemental firing make it attractive for retrofit solar augmentation. Only minimal interface or integration requirements are envisioned, with no alterations to the gas turbine or steam cycle machinery.

A diagram illustrating a possible method of integrating a solar heat receiver with the exhaust stack of an open cycle gas turbine is presented in figure 14. The prime energy source for the heat recovery steam generator (HRSG) would remain the gas turbine exhaust stream assuming the

temperature required for solar supplemental firing equivalent to that utilized for current fossil-fuel-fired HRSG's. This temperature need not exceed  $760^{\circ}\text{C}$  ( $1400^{\circ}\text{F}$ ) to produce  $9.1 \times 10^4$  kg/hr ( $2 \times 10^5$  lb/hr) of  $6.2 \text{ MN/m}^2$  (895 psi),  $446^{\circ}\text{C}$  ( $830^{\circ}\text{F}$ ) steam (ref. 4) and can be accomplished using current state-of-the-art metal heat exchangers. Also, these temperature levels should provide good solar utilization and fuel savings indicating a good potential for economic feasibility of this concept in a retrofit application.

### c. Component and System Considerations

The following discussion pertains to various design and operational aspects of simple, recuperated and combined gas turbine cycle components and systems. These comments include synopses of discussions held with various members of an advisory panel as well as findings of the authors. They are intended to illuminate many of the technical problems related to a solar thermal hybrid gas turbine system, and thereby to indicate some direction for future efforts in this area.

#### Compressor Technology

The most recently developed compressors for gas turbine cycle power-plant application have polytropic stage efficiencies approaching 92 percent. Stages are very lightly loaded for long-life operation. Compressors are stacked (e.g., a low pressure compressor feeding a high pressure compressor) to produce a high system CPR. Therefore, in a new or advanced system design of a recuperated gas turbine cycle, it may be possible to integrate the low pressure compressor of a current system into the advanced design to provide the optimum CPR, at a high compressor efficiency.

Aircraft engine manufacturers have achieved compressor stage efficiencies of about 95 percent by bleeding off some high temperature (high friction) flow from the compressor tip region. Should compressor inter-cooling appear feasible as a means of improving thermal cycle efficiency, it may be combined with such a bleed for optimum benefit.

Intercooling would probably not be feasible with a low CPR machine since a relatively small amount of internal heat is added to the cycle. A thermodynamic analysis would ascertain the minimum CPR for effective intercooling.

### Combustor Technology

Emission of oxides of nitrogen,  $\text{NO}_x$ , decrease with decreasing CPR. Hence, recuperated gas turbine hybrids operating at low CPR's should produce less  $\text{NO}_x$  during periods of fuel combustion.

Conventional combustor liners are cooled by compressor discharge air. With the trend towards higher combustor inlet and exit temperatures, liner temperatures are increasing, thus affecting the durability and life of the liner. When the average inlet temperature reaches about  $649^\circ\text{C}$  ( $1200^\circ\text{F}$ ), portions of the liner will have approached  $871^\circ\text{C}$  ( $1600^\circ\text{F}$ ). This is the maximum wall temperature that can be maintained in order to avoid oxidation and degradation of strength. Hence for series arrangement of solar/fossil fuel heat inputs, a development program would be required to determine new or improved techniques of combustor cooling. For this reason, solar/fossil hybrid systems with a series arrangement of heat inputs is not currently feasible. Possible alternatives to conventional combustors are ceramic combustors and catalytic reactors which are currently under study in advanced aircraft and automotive development programs.

A parallel arrangement of solar/fossil fuel heat inputs is feasible for solar hybrid systems as long as the temperature of the solar heat exchanger outlet is consistent with the energy level into the turbine. Should the solar heat exchanger temperature level decrease significantly, operation would necessarily switch to a fossil-fuel-only mode if the energy level into the turbine is to be maintained. In the parallel arrangement, development efforts should be directed toward combustors which can produce a surplus of energy to supplement the solar heat input, as well as to solar heat exchanger/fossil fuel combustor controls. Here again, possibilities exist for the use of ceramic combustors and catalytic reactors, as well as for induct afterburning upstream of the turbine.

Catalytic combustors have favorable characteristics for advanced solar thermal hybrid system designs with a series arrangement of solar/fossil fuel heat inputs. They require a mixture of preheated air and fuel for proper reaction, and they have very low emission levels. However, additional technical effort is needed to develop this type of combustor for gas turbine application, particularly from the standpoints of design complexity, maintenance required, response time, and auto-ignition with premixed flow.

### System Dynamics and Controls

From a controls standpoint, a series arrangement of solar heat exchanger and fossil fuel combustor would present the fewest problems. In a parallel arrangement, the pressure drop across both the solar heat exchanger and the fossil fuel combustor must be controlled independently.

Bypass lines across the turbine(s) are needed to control synchronous speed. With the additional complexity of a solar thermal hybrid system, this remains the main control problem of the system.

Emergency transient controls, synchronous speed controls, and solar and fossil fuel heat input controls all require some further degree of study for an advanced system design.

### Turbine Technology

Gas turbine technology has attained a high level of sophistication. Still, R and D is continuing in several areas, including efforts to improve overall turbine efficiency, develop more refined methods of high temperature cooling, improve hot corrosion resistance, and extend cyclic fatigue life. Of these, turbine sensitivity to cyclic fatigue is potentially the most serious problem associated with a solar thermal hybrid system.

### Heat Exchanger Technology

High temperature solar gas heat exchanger technology has one of the highest priorities of solar thermal R and D. Although a thorough discussion

of this subject is outside the scope of this study, some comment on the status of this effort is pertinent. Current metallurgical constraints limit the gas temperature exiting the heat exchangers to about  $760^{\circ}\text{C}$  ( $1400^{\circ}\text{F}$ ). Technology is currently being developed to increase this temperature by using ceramic heat exchangers (ref. 5). For a solar/fossil series configuration, however, development of heat receivers capable of providing high temperature is desirable but not necessary because of fossil fuel augmentation.

The recuperator represents a major cost item of the open-cycle gas-turbine system. The design parameter having the greatest effect on recuperator size, and therefore cost, is the effectiveness. Yet, the cost of a solar thermal hybrid system is heavily dependent on the size of the solar collector field employed, which in turn is inversely related to the thermodynamic efficiency of the cycle. Hence a detail design of a solar thermal hybrid system using a recuperated gas turbine cycle would require an optimization study to select the recuperator effectiveness which results in the lowest cost of electricity (COE).

### System Operation

Various modes of system operation can be employed to improve overall system efficiency. The use of one or more stages of reheat will effectively increase the temperature at which heat is added to the cycle, thereby increasing cycle efficiency. Similarly, the use of one or more stages of compressor intercooling will effectively lower the temperature at which heat is rejected, thereby also increasing cycle efficiency. Some discussion of intercooling has already been presented in the subsection Compressor Technology. In general, this method of improving efficiency would not be feasible with a low CPR machine (e.g., CPR = 4:1). However, a recent study (ref. 6) of intercooling in a recuperated gas turbine cycle with an intermediate CPR of 10:1 showed an 8 percent improvement in cycle efficiency and a 6 percent decrease in COE.

The potential improvement in thermal cycle efficiency due to reheat must be balanced with additional losses incurred in combustion and exhaust processes. An assessment of these trade-offs was made in the study reported in

reference 7. In contrast to intercooling, these cycle studies indicated only marginal benefits from reheat. Hence no further consideration was given to this mode of operation in this study.

#### d. VAPOR CYCLES

The initial effort to determine the technical feasibility of solar augmentation of vapor cycles was an investigation of solar displacement of the input energy requirements for retrofit of conventional fossil-fueled steam powerplants. The purpose of this exercise was to determine the maximum possible solar augmentation for specific thermal energy input (i. e. , temperature) points in a conventional vapor cycle. In addition, it was also desired to assess the effect of cycle peak pressure on the maximum solar energy utilization. The results of these calculations are shown for two typical modern steam powerplants in table III. The two plants evaluated have normal full load steam conditions of  $8.3 \text{ MN/m}^2$  (1200 psig),  $538^\circ \text{ C}$  ( $1000^\circ \text{ F}$ ) superheat/ $538^\circ \text{ C}$  ( $1000^\circ \text{ F}$ ) reheat, and  $16.6 \text{ MN/m}^2$  (2400 psig),  $538^\circ \text{ C}$  ( $1000^\circ \text{ F}$ )/ $538^\circ \text{ C}$  ( $1000^\circ \text{ F}$ ), respectively. The energy input requirements were calculated for the following cycle points: feedwater heating, preheating, evaporation, superheating, and reheating. Also shown in table III are the energy requirements for combined evaporation and superheating. The effect of decreasing pressure level from  $16.6 \text{ MN/m}^2$  (2400 psig) to  $8.3 \text{ MN/m}^2$  (1200 psig) on the energy requirements for these plants is seen to have negligible effect on both feedwater heating and reheating, a moderate effect (20 percent decrease) on superheating, and a major effect on preheating (60 percent decrease) and evaporation (90 percent increase). For the combination of evaporation and superheating the net effect is a 30 percent increase in energy input. In addition, the highest percentages of energy input occur in the boiler which includes the requirements of preheating, evaporation, superheating, and reheating.

An early study (ref. 8) of seven methods of absorbing solar energy into a  $16.6 \text{ MN/m}^2$  (2400 psig)/ $538^\circ \text{ C}$  ( $1000^\circ \text{ F}$ )/ $538^\circ \text{ C}$  ( $1000^\circ \text{ F}$ ) steam Rankine powerplant concluded that both solar augment of combined evaporation and superheating and solar augment of feedwater heating were preferred methods.



That study also concluded that of the two preferred methods, combined evaporation and superheating had a net useful solar capacity to gross solar input ratio of 100 percent while the ratio for feedwater heating was limited to 68 percent. A ratio of less than 100 percent indicates that the overall thermal efficiency of the plant is degraded by solar augmentation, and that, in effect, some of the solar heat input is wasted. The ratio of net useful solar capacity to gross solar input is therefore a measure of the solar fuel saving efficiency of the solar augmentation method used. A solar fuel saving efficiency may, therefore, be defined as the ratio of fuel saved to solar energy input. A more recent study of the feasibility of solar augmentation of boiler feedwater heating (ref. 9) provides more detail on solar fuel saving efficiency. The assumption of constant plant output leads to a simple approximation of fuel saving efficiency as a function of plant heat rate and extraction steam enthalpy. The fuel saving efficiency for solar augmentation at various points in a feedwater heating chain was calculated in order to determine the optimum point for solar input. The results are shown in figure 15. The solar fuel saving efficiency is plotted as a function of solar heat input location in terms of extraction steam enthalpy and feedwater heater exit temperature state points for three plant heat rates. The low heat rate is representative of a modern plant, the high heat rate represents an older plant, and the intermediate value is an estimate of the average plant heat rate for oil and gas-fired steam plants in the U. S.

The solar fuel savings efficiency is shown to increase as the value of the replaced extraction steam enthalpy and feedwater temperature increases. In addition, the fuel saving efficiency of solar augmentation increases as plant efficiency decreases. In general, solar augmentation is most effective in conserving energy in high-temperature feedwater heaters in older plants with high heat rates. The numerical results presented show the maximum net useful solar capacity for the highest temperature feedwater heater considered ( $249^{\circ}\text{C}$ ) varies from 65 percent to 93 percent depending on plant heat rate. The value of 68 percent reported in reference 8 was based on a modern high efficiency plant and compares well with the values calculated in reference 9 for the low plant heat rate case.

A variety of possible solar augmentation methods is possible in a typical steam powerplant for both feedwater heating and combined evaporation and superheating. The following discussion will be limited to these two cycle input points based on their high solar utilization and on the more detailed examination of design complexity, operation, control, and cost estimates given in references 8 and 9.

Basically, one may solar augment a desirable cycle input point with either a series or parallel method. Each configuration will have both advantages and disadvantages that will be peculiar to the pressure and temperature of the cycle input point considered. In addition, since most steam plants have differing and sometimes unique design and control features, it is unlikely that a generic method will be optimum for all. However, several conclusions appear to be relatively independent of plant designs.

With respect to solar augmentation of feedwater heating the following comments are applicable:

(1) A series configuration will generally eliminate flow control problems provided that a conventional feedwater heater is upstream of the solar heat exchanger as shown in figure 16. The recommended location for solar energy input in a series configuration would be before the last feedwater heater to achieve maximum fuel savings.

(2) A parallel configuration will provide a modest increase in fuel savings (over the series arrangement) provided that the solar input is upstream of the last feedwater heater, i. e., economizer inlet, as shown in figure 17. According to reference 9 this configuration requires the addition of a separate high pressure feedwater pump and a provision for extraction steam bleed (to minimize thermal transients) to the bypassed feedwater heaters.

For solar augmentation of combined evaporation and superheat, the following comments are applicable:

(1) A parallel configuration using a twin furnace design appears to be a reasonable scheme although some design complexity is inherent in this method. Control of flue gas to the reheater and control of solar superheated steam temperature are required. This method was recommended in reference 8 and is shown in figure 18.

(2) A combination of parallel solar augment of feedwater heating and combined evaporation and superheating functions utilizing a single solar heat exchanger appears worthy of further investigation.

(3) A thermal model of hybrid steam cycle plants has been developed (ref. 10) and should allow a determination of plant response characteristics as well as define operating limitations.

In summary, the technical feasibility of solar augmentation of vapor cycle powerplants appears reasonable from the standpoints of plant integration and theoretical (maximum) fuel savings. The more practical aspects of solar integration as well as realistic estimates of fuel savings are largely unanswered at this time. One point relative to fuel savings for solar augmentation of combined evaporation and superheat is that a fossil-fuel-fired boiler may be throttled down to only about 30-50 percent of steam flow. This indicates that a parallel solar evaporator and superheater can achieve only one-third to one-half of the maximum fuel savings possible. Another point is that the maximum fuel savings from any mode of solar augmentation to an existing plant will require a detailed heat balance analysis for that plant. Based on the results presented in table III, it appears that lower pressure plants offer the potential for increased fuel savings. However, the effect of feedwater temperature is quite important as was shown in figure 15. Therefore, the feasibility of solar retrofit to existing plants with, say, both low pressures and low final feedwater and superheat temperatures must be assessed on an individual basis.

Areas of required technology development have been identified in references 8 and 9. These are as follows:

1. Hybrid system off-design capability for steady state and transient operation.
2. Superheat control of the vapor from parallel solar and fossil boilers.
3. Feedwater heating loop flow control.

## 2. ECONOMIC ANALYSIS

The economics of solar thermal systems is an important criterion for determining the acceptance of these systems by the utility industry and other potential users. The market capture potential of any solar thermal system can be estimated by comparative economic evaluation with conventional fossil and nuclear powerplants. The overall purpose of this analysis was to parametrically examine the first order economics, on a consistent basis, to identify the general regimes of economic viability of solar thermal systems. A secondary objective of the analysis was to identify specific solar/fossil hybrid system combinations that show economic attractiveness when compared to solar standalone, and solar with energy storage systems.

The details of the methodology used to generate the results presented in this section are given in appendix E. The results of the economic analysis are presented in following subsections:

- a. Comparative Economics of Powerplant Types
- b. Variation of Solar Thermal Energy Collection Subsystem Cost
- c. Variation of Cost of Fuel
- d. Variation of Hybrid Cost of Integration

### a. Comparative Economics of Powerplant Types

An economic comparison of hybrid and solar thermal with storage powerplants is shown in figure 19. Also shown for comparison are three representative operating point cost estimates for conventional utility powerplants. The comparison is presented on a cost-of-electricity (COE) versus plant capacity factor basis in 1975 dollars. An 18 percent fixed charge rate was used for the capital portion of COE. Also indicated on the abscissa is an overlay of average daily storage capacity time for solar plants using storage. These times also represent the average daily fossil fuel "burn" time for hybrid plants using fuel instead of energy storage. The net useful daily solar operating time was assumed to be seven hours which is equivalent to an annual (solar) plant capacity factor of 0.29. The cost input parameters used to generate the comparison are shown in table IV.

The capital costs for all solar energy collection subsystems were assumed to be \$833/kJ/sec (\$28/M Btu/yr). This is equivalent to an installed solar collection cost of about \$150/m<sup>2</sup> (\$15/ft<sup>2</sup>) in a southwest U. S. location. All hybrid systems were assumed to utilize fossil fuel at a cost of \$2.37/GJ (\$2.50/M Btu) - the approximate cost of 1977 imported fuel oil. Solar thermal systems utilizing energy storage are shown for low and high storage cost estimates - \$8.3/MWe sec (\$30/kWe hr) and \$27.8/MWe sec (\$100/kWe hr), respectively.

The results of this parametric comparison, presented in figure 19, show that solar/fossil hybrid systems exhibit a COE that is considerably lower than solar systems utilizing energy storage, and that advanced, high efficiency hybrid systems can compete with conventional utility powerplants in the intermediate load regime.

#### b. Variation of Solar Thermal Energy Collection Subsystem Cost

The effect of varying the solar thermal energy collection subsystem cost from \$208/kJ/sec (\$7 M Btu/yr) to \$1666 kJ/sec (\$56/M Btu/yr) is shown in figure 20 for a hybrid powerplant. The powerplant used in this illustration is represented by a \$150/kWe simple cycle gas turbine. The overall effect of reducing solar subsystem cost is significant for this powerplant. For example, the cost of electricity is reduced 30-40 percent when solar subsystem costs are halved. Also shown for comparison is the COE for a conventional utility plant. A solar collection cost of about \$10/M Btu or \$6/ft<sup>2</sup> (S. W. U. S. location) is needed to match conventional plant COE's.

The effect of varying solar subsystem cost for a solar thermal plant with energy storage is shown in figure 21. For convenience, hours of storage capacity are shown along with capacity factor. The powerplant used in this illustration is represented by a \$600/kWe steam Rankine cycle with a low-cost energy storage subsystem. The results shown in figure 21 dramatically illustrate the high cost of electricity for solar storage powerplants. The variation of solar thermal energy collection subsystem cost on cost of electricity is also significant for this type plant. For example, at a plant

capacity factor of 0.5, reduction of solar subsystem costs from \$1666/kJ/sec (\$56/M Btu/yr) to \$833/kJ/sec (\$28 M Btu/yr) decreased the cost of electricity by 40 percent. Reduction from \$833/kJ/sec (\$28/M Btu/yr) to \$416/kJ/sec (\$14/M Btu/yr) decreased the cost of electricity by 30 percent. The last factor-of-two reduction to \$208/kJ/sec (\$7/M Btu/yr) decreased the cost of electricity by 20 percent. However, these plants cannot compete with conventional utilities at any solar collection cost.

An important aspect of the total solar energy collection cost for solar plants utilizing energy storage is not fully illustrated in these results. This is simply the increased energy collection area and land area required due to the additional inefficiency of any storage method. The ratio of required solar collection area for a plant with energy storage to one without storage, as a function of storage efficiency and discharge time to charge time ratio is shown in figure 22. The figure indicates the significant collector area, and therefore cost, penalties associated with thermal energy storage systems. With a typical storage overall efficiency of 60 percent and a charge/discharge ratio of 0.6 the required area for a plant with storage is more than 3.5 times that for a hybrid plant without energy storage. The corresponding increase in cost of electricity is even higher due to the additional cost of the storage subsystem itself. Also, the larger land areas required for plants with energy storage may limit implementation in some locations.

### c. Variation of Cost of Fuel

The effect of varying the cost of fuel for hybrid and conventional utility combined cycle powerplants is shown in figure 23. Fuel cost values of \$2.37/GJ (\$2.50/M Btu) and \$3.80/GJ (\$4.00/M Btu) were chosen.

The hybrid powerplant used for this illustration has an energy conversion cost of \$370/kWe of which \$70/kWe is assumed for hybrid integration costs. The conventional utility powerplant shown has a total capital cost of \$243/kWe. Solar energy collection costs of \$416 kJ/sec (\$14/M Btu/yr) were assumed for the hybrid powerplant. This is equivalent to an installed collection cost of about \$80/m<sup>2</sup> (\$8/ft<sup>2</sup>) in a southwest U.S. location.

Comparison of these particular hybrid and conventional plants at capacity factors of 0.45 and 0.65, shows that the conventional plant can provide lower cost of electricity at fuel costs of \$2.37/GJ (\$2.50 M Btu). However, when fuel costs rise to \$3.80/GJ (\$4.00/M Btu) the hybrid combined cycle power-plant can produce electricity at lower cost than representative conventional plants in the intermediate load regime, and show a breakeven point at baseload. In general, since hybrid plants typically require less fuel than conventional plants they will show a COE advantage with increasing fuel costs.

#### d. Variation of Hybrid Cost of Integration

The effect of varying the hybrid plant integration cost is shown in figure 24. Six cases, representing two hybrid types and three integration costs are presented.

Curves A, B, and C of figure 24 show the effect of adding integration costs of \$10/kWe, \$70/kWe, and \$140/kWe, respectively to an oil-fired hybrid gas turbine plant with a capital cost of \$150/kWe. The cost penalty for intermediate and baseload operation is only about 10 percent for each jump in integration cost for this type plant. Curves D, E, and F show the effect of adding the same three integration costs to a \$600/kWe oil-fired steam Rankine plant. The results show a lower cost penalty of about 5 percent for each integration cost increase throughout the intermediate and baseload regime.

### SUMMARY OF RESULTS

A preliminary feasibility study of hybrid solar thermal systems was conducted to evaluate the overall technical and economic aspects of this class of solar electric power system. The hybrid systems considered in this study utilize fossil fuel in combination with solar energy to provide thermal input to an energy conversion subsystem. Current solar thermal concepts use solar energy in combination with thermal energy storage to provide input to a steam Rankine energy conversion subsystem. The energy conversion subsystems considered in this study included steam

Rankine cycles plus simple and recuperative open cycle Brayton and combined (steam and gas) cycles as well. The following overall results were obtained:

1. The cost of electricity (COE) of solar/fossil hybrid systems was found to vary within a range bounded by solar/thermal energy storage systems and conventional fossil fuel powerplants. For example, a hybrid gas turbine system operating for 13 hours per day (7 hr solar, 6 hr fossil fuel) exhibited a range of COE from 30 mills/kW hr to 60 mills/kW hr for solar collection costs ranging from \$80/m<sup>2</sup> to \$300/m<sup>2</sup>. For the same daily capacity a solar steam cycle thermal energy storage system with a 6 hour storage capacity at \$8.3/MWe sec (\$30/kWe hr) yielded a COE of 80 mills/kWe hr at a solar collection cost of about \$150/m<sup>2</sup>. A conventional steam cycle powerplant operating at a 0.54 capacity factor (13 hr/day) would yield a COE of about 27 mills/kWe hr (1975 dollars).

2. Significant solar thermal powerplant capital cost reductions can occur through increase of energy conversion efficiencies that reduce solar collector area requirements for a given power output. New and advanced hybrid systems that combust fossil fuel as a temperature augment to solar energy input can utilize high temperature, efficiency-optimized energy conversion systems at reasonably modest solar input temperatures. For example, recuperated gas turbine energy conversion subsystems can achieve 44 percent efficiency, and efficiencies of 46 to 50 percent are achievable with combined cycle (gas turbine/steam Rankine) systems - using current state-of-the-art solar receiver, recuperator, and turbine technology.

3. Significant reduction of solar collector field area, and therefore, plant capital cost, is a benefit that accrues from the use of hybrid systems. Hybrid systems eliminate the need for long-term energy storage and the associated solar collector area required to charge the storage subsystem and, in addition, would not be paced by the development time of thermal energy storage subsystems. A solar plant incorporating a typical thermal energy storage subsystem with a charge/discharge ratio of 0.6 and a storage efficiency of 60 percent would require a solar collection area more than 3.5 times larger than that required for a hybrid powerplant. In terms of overall system capital cost, a range of reduction factors of 2.25 to 2.75 would occur for hybrid solar collection subsystem cost fractions of 50 percent to 70 percent, respectively.



4. Technical feasibility of solar hybrid retrofit of existing fossil-fired steam Rankine powerplants was confirmed. The economic feasibility of hybrid retrofit was found to be dependent upon the thermodynamic characteristics of the specific (existing) powerplant considered as well as the cost of solar energy collection. Low system pressures, high final feedwater temperatures, and high plant heat rates all contribute to increased fuel savings and therefore economic feasibility. Technology advancements are required in the areas of off-design capability for transient operation and flow control of both boiler superheat and feedwater heating loops.

5. Retrofit hybrid solar thermal concepts that utilize fossil fuel to augment solar energy input temperatures into Brayton cycle gas turbines can provide fuel savings benefits over conventional powerplants. These benefits accrue from both the displacement of fossil fuel by solar energy and the increased efficiency of fuel use at temperatures above solar energy input values. The fuel savings benefits due to solar displacement were found to be dependent on solar energy input temperature, peak temperature of the energy conversion cycle, and cycle type. For example, at an average solar input temperature of  $760^{\circ}\text{C}$  ( $1400^{\circ}\text{F}$ ) to a simple cycle gas turbine operating at  $982^{\circ}\text{C}$  ( $1800^{\circ}\text{F}$ ) peak cycle temperature, a solar fraction of 60 percent and a fuel savings of about 6500 Btu/kWe hr was determined. For an annual solar operation of 3000 hours and a projected fuel cost of \$2.84/GJ (\$3.00/M Btu) the solar fuel savings is about \$59/kWe or about \$6 million per year for a 100 MWe powerplant. In terms of national impact, if half of the existing domestic peaking combustion turbine capacity could be retrofit and operated as described, an equivalent of 80 million barrels of oil could be saved annually.

## SYMBOLS

CPR	compressor pressure ratio, dimensionless
G	billion ( $10^9$ )
HHV	higher heating value, 43.5 MJ/kg (18 700 Btu/lb)
k	thousand ( $10^3$ )
M	million ( $10^6$ )
P	pressure, $\text{N/m}^2$ (psia)
Q	rate of heat flow, W (Btu/hr)
T	temperature, $^{\circ}\text{C}$ or K ( $^{\circ}\text{F}$ or $^{\circ}\text{R}$ )
TIT	turbine inlet temperature, $^{\circ}\text{C}$ or K ( $^{\circ}\text{F}$ or $^{\circ}\text{R}$ )
$\gamma$	specific heat ratio, dimensionless
$\epsilon$	recuperator effectiveness, dimensionless
$\eta$	efficiency, dimensionless

## Subscripts:

A	solar heat into receiver
B	fossil heat into combustor
C	recuperator hot to cold side
D	gas exhaust into steam cycle
1	ambient or compressor inlet
2	compressor outlet or recuperator inlet
3	recuperator outlet or solar receiver inlet
4	solar receiver outlet or combustor inlet
5	combustor outlet or gas turbine inlet
6	gas turbine outlet or recuperator inlet
7	recuperator outlet or stack heat exchanger inlet
8	stack exhaust

9 steam cycle turbine inlet

10 steam cycle outlet

Superscript:

' alternate flow or heat input path

Abbreviations:

COND condenser

ECON economizer

EVAP evaporator

FWH feedwater heater

HP high pressure

HX heat exchanger

IP intermediate pressure

LP low pressure

SH superheater

APPENDIX A

NASA-LEWIS TASK TEAM

Harvey Bloomfield - Team Leader

James Calogeras

Vernon Gebben

Kent Jefferies

William Beede

Charles Younger

APPENDIX B

DISCIPLINES REPRESENTED BY NASA-LEWIS ADVISORY PANEL

System Dynamics and Controls

Compressors

Combustors

Stationary Power Systems

Gas Turbines

Heat Exchangers

ECAS Systems Analysis

## APPENDIX C

## LIST OF SOURCE CONTACTS

Aerospace Corporation  
Boeing Company  
Black and Veatch Consulting Engineers  
Burns and Roe, Inc.  
Colorado State University  
Electric Power Research Institute  
Foster Wheeler Corporation  
Franklin Institute  
General Electric Company  
Honeywell, Inc.  
Jet Propulsion Laboratory  
Public Service Co. of Arizona  
Public Service Co. of New Mexico  
University of Houston  
Westinghouse Corporation

## APPENDIX D

## TECHNICAL ANALYSIS METHODOLOGY

## 1. Simple and Recuperated Gas Turbine Cycles

An evaluation was made of the technical feasibility of an open cycle gas turbine powerplant concept that could operate with both solar and fossil fuel thermal inputs. During periods of sunlight, the fossil fuel could augment the solar heat input to maintain a constant turbine inlet temperature (as required). Night time operation is possible with fossil fuel as the sole source of thermal input.

Three types of gas turbine cycles were included in this study. A simple cycle was considered in which waste heat from the turbine was vented to the atmosphere through an exhaust stack. A regenerative cycle was considered in which compressor pressure ratio was optimized as a function of recuperator effectiveness. And a combined cycle was considered in which the gas turbine cycle, either simple or recuperated, served as the topping cycle to a steam Rankine bottomer. Both unfired and supplementally-fired combined cycles were included in this consideration.

The technical evaluation was both quantitative and qualitative in nature. A computer code was written to make parametric variations in compressor pressure ratio, peak cycle operating temperature, solar energy input temperature and recuperator effectiveness for each of the cycle types. Cycle efficiency was computed for each parametric case, including that case in which compressor pressure ratio corresponded to maximum cycle efficiency. The code incorporated routines involving fossil fuel savings, required solar and fossil fuel heat inputs, component efficiencies, ducting and stack losses, and atmospheric conditions.

Consideration was given to one or more stages of reheat and compressor intercooling as methods of improving overall cycle efficiency. Operation with the solar receiver or heat exchanger in parallel with the fossil fuel combustion chamber, rather than in series, was also considered.

One aspect of this study is significant and deserves further discussion. In the consideration of each of the solar hybrid concepts, and parametric

variations thereof, an approach was taken to maximize overall thermal cycle efficiency. Typically, designs of conventional fossil-fueled gas turbine powerplants have taken an approach that maximizes specific power. These designs result in a favorable cost-of-electricity (COE) associated with plants of relatively small-sized components producing power at a nominal efficiency, rather than larger plants producing the same amount of power at higher efficiency.

But the cost-effectiveness of a solar hybrid plant is largely dependent on size of the associated solar collector field. Since collector field size is inversely proportional to overall cycle efficiency, a decision was made at the outset of this study to maximize the overall cycle efficiency.

For simple cycle (unrecuperated) operation, ideal thermal cycle efficiency is related only to compressor pressure ratio (CPR) and the ratio of specific heats ( $\gamma$ ) as follows:

$$\eta_{\text{ideal}} = 1 - \frac{1}{(\text{CPR})^\alpha} \quad \text{where } \alpha = \frac{\gamma - 1}{\gamma} \quad (1)$$

Equation (1) is plotted in figure D1 for ratios of specific heats equal to 1.4 and 1.35.

The significance of equation (1) (and figure D1), is that for an open cycle gas turbine system without a recuperator, the ideal thermal cycle efficiency tends to continuously increase with pressure ratio. It is the peak cycle operating temperature that ultimately restricts CPR. In turn, the peak cycle operating temperature is limited by turbine and combustor materials properties. This is described schematically in figure D2.

The solid lines of figure D2 correspond to an initial cycle operation with a lower CPR. The dashed lines correspond to a cycle with the same ambient and peak temperatures, but with a higher CPR. Although ideal cycle efficiency may be higher in the latter case, the ability to produce work has been lessened because the maximum temperature limitation restricts the amount of external heat that may be added to the cycle to produce work.



The restriction on external heat addition to a simple cycle with a higher CPR is compounded when component efficiencies are taken into account. Friction losses, particularly in the compressor, increase significantly with CPR. Compressor friction results in increased internal heat, further restricting external heat addition. Hence the actual thermal cycle efficiency reaches a maximum at some value of CPR then decreases with a further increase in CPR.

For recuperated cycle operation, ideal cycle efficiency is related to peak cycle operating temperature, ambient temperature, and recuperator effectiveness ( $\epsilon$ ), as well as CPR and  $\gamma$ . This relationship is readily derived and is given in equation (2) and presented in figure D3 for a temperature ratio ( $T_1/T_5$ ) of 4.0 and  $\gamma = 1.4$ .

$$\eta_{\text{ideal regenerative}} = \frac{\left[ (\text{CPR})^\alpha - 1 \right] \left[ (\text{CPR})^{-\alpha} - \frac{T_1}{T_5} \right]}{1 - \epsilon (\text{CPR})^{-\alpha} + (\epsilon - 1) \frac{T_1}{T_5} (\text{CPR})^\alpha} \quad (2)$$

where

$$\alpha = \frac{\gamma - 1}{\gamma}$$

When  $\epsilon = 0$  (unrecuperated) equation (2) reduces to the simple cycle relationship given in equation (1).

Several aspects of equation (2) and figure D3 have direct bearing on this study. The first is that ideal cycle efficiency is significantly improved by the addition of a recuperator, and that the improvement is proportional to the effectiveness ( $\epsilon$ ) of the recuperator. (Indeed, for the hypothetical case of  $\epsilon = 1.0$  at  $\text{CPR} = 1:1$ ,  $\eta_{\text{ideal}} = \eta_{\text{Carnot}}$ ).

Another relevant point is that the region of the "knee" of the curve of  $\eta_{\text{ideal}}$  versus CPR, (i. e., that region where the slope changes most rapidly), moves toward lower CPR's as recuperator effectiveness increases.

A fundamental difference, then, between a simple open cycle gas turbine system and a recuperated system optimized for high efficiency is in the compressor pressure ratio. Currently the most advanced simple cycle systems being developed for power generation utilize compressors which produce as high as 16:1 pressure ratios. A recuperated system designed within the same boundary conditions would utilize a compressor with a CPR of perhaps 4:1 for maximum thermal efficiency.

The major emphasis of the quantitative analysis was to determine the CPR which resulted in maximum thermal cycle efficiency for both the simple cycle and the recuperated cycle. CPR's were varied from 2:1 to 20:1 over a range of peak cycle operating temperatures from 982° C (1800° F) to 1204° C (2200° F) and a range of recuperator effectivenesses from 0 to 0.95. Within the limits of compressor discharge temperature and turbine inlet temperature (i. e., peak cycle operating temperature), the maximum solar input temperature was varied from 482° C (900° F) to 1204° C (2200° F), in steps of 38° C (100° F). A temperature of 16° C (60° F) and a pressure of 101.4 KN/m<sup>2</sup> (14.7 psia) were assumed for ambient conditions.

Pressure losses of 3-percent each were assigned to the cold-side recuperator (for the recuperated cycle), the solar heat exchanger and the fossil fuel combustion chamber. Pressure losses of 1-percent were assigned to the hot-side recuperator and to the exhaust stack. The cumulative pressure loss for the simple cycle system was about 7 percent. For the recuperated cycle system, cumulative pressure loss was about 11 percent. These losses are representative of state-of-the-art component design.

To be compatible with the economic analysis, each parametric cycle calculation was assumed to produce a net power output of 1.0 kWe. A higher heating value (HHV) of 43.5 MJ/kg (18 700 Btu/lbm) was used in conjunction with the fossil fuel thermal input to determine net savings of fossil fuel due to solar hybrid operation. This corresponds to an approximate value for number 6 fuel oil.

## 2. Combined Cycles

A relation for combined cycle thermal efficiency was obtained as a function of gas turbine cycle efficiency and recuperator discharge temperature,  $T_7$  (or turbine discharge temperature for the simple cycle). This relation was based upon the following conditions:

$$T_1 = 289^\circ \text{ K } (520^\circ \text{ R})$$

$$T_4 = 1256^\circ \text{ K } (2260^\circ \text{ R})$$

$$T_5 = 1256, 1310, 1366, 1478^\circ \text{ K } (2260, 2360, 2460, 2660^\circ \text{ R})$$

$$T_8 = 422^\circ \text{ K } (760^\circ \text{ R})$$

$$T_9 = T_7 - 55.5^\circ \text{ K } (T_7 - 100^\circ \text{ R})$$

$$Q_D = 90 \text{ percent of ideal transfer (10 percent energy lost to environment)}$$

$$P_9 = 12.4 \text{ MN/m}^2 \text{ (1800 psi)}$$

An estimation of steam Rankine cycle efficiency was made from overall efficiency data (ref. 1) for a 500 MWe steam powerplant. This estimation is presented in figure D4. The points correspond to  $24.2 \text{ MN/m}^2$  (3500 psi) and  $16.6 \text{ MN/m}^2$  (2400 psi) data from reference 1. The dashed line is an extrapolation of these data to the assumed steam pressure of  $12.4 \text{ MN/m}^2$  (1800 psi).

The estimated steam Rankine cycle curve of figure D4 was used to couple recuperator discharge temperature,  $T_7$ , with gas turbine cycle efficiency in order to calculate the combined cycle efficiency. This estimation is considered representative of an  $12.4 \text{ MN/m}^2$  (1800 psi) steam pressure powerplant at peak cycle operating temperatures above about  $427^\circ \text{ C}$  ( $800^\circ \text{ F}$ ). At temperatures below this level, the pressure of saturated steam would necessarily be lessened to maintain steam quality in the turbine. Corresponding steam powerplants would achieve thermal efficiencies somewhat lower than those indicated by the estimated curve (fig. D4). Combined cycle efficiencies, in turn, would be somewhat lower than those indicated in this analysis.

## APPENDIX E

## ECONOMIC ANALYSIS METHODOLOGY

The economic analysis methodology developed for conducting the comparative assessments is shown symbolically in figure E1. A digital computer program was developed to determine the relative busbar cost of electricity for four basic powerplant types: (1) solar standalone - this plant operates only during a portion of the available sun hours, power output varies with time; (2) conventional fossil or nuclear powerplant - can operate up to 24 hours per day; (3) solar/fossil hybrid - this plant utilizes all the solar energy it can collect, power output can be provided up to 24 hours per day, and (4) solar with thermal energy storage - this plant also utilizes all the solar energy it can collect. Power output time is restricted only by the limit of energy storage time (capacity) desired.

The powerplant operational methodology developed was based upon the ground rules indicated in figure E1. These assumptions were required to evaluate the four powerplant types on a consistent basis. For a normalized solar plant power output of 1 kWe the solar portion of any powerplant must generate a minimum of 7 kWe hr on an annualized average day. The remaining 17 kWe hr or any portion thereof can be generated by either the fossil-burning portion of a hybrid plant or the energy storage portion of a solar with storage plant. This assumption is illustrated in figure E2 which depicts the average day operation for all plant types. An average day insolation period of 12 hours is indicated for a typical site in the U. S. southwest.

It is important to note that a 7 kWe hr solar standalone plant cannot provide a 1 kWe power output on the average day, while the solar plus 6 hour storage plant illustrated must have a solar capacity equivalent to 13 kWe hr in order to produce 1 kWe on the average day.

Another key assumption, necessary to a consistent evaluation of powerplant types, was that all solar plants will generate their maximum output power from solar input alone at noon on the summer solstice. An illustration of how this assumption compares to the average day and the winter solstice condition is shown in figure E3 for a solar/fossil hybrid powerplant.

For the particular powerplant type of interest the computer program will calculate relative busbar cost of electricity based upon the input cost parameters desired. A listing of input cost parameters investigated is shown in table E2. These will be discussed in more detail in the following sections.

### Cost Parameters

#### a. Energy Conversion Subsystem Type/Cost

A wide range of energy conversion costs, from \$150/kWe to \$800/kWe, in 1975 dollars was studied to bracket a variety of fossil and nuclear types. For conventional plants, this cost is the total installed powerplant cost.

#### b. Solar Thermal Energy Collection Subsystem Cost

The estimated cost of collecting solar energy includes collectors, support structure, piping, tower (if required) and installation, and has been expressed in units of dollars per energy collected per year. Using these units allows this analysis to be independent of specific collector site, cost, and efficiency inputs. This cost parameter is equivalent to the product of three factors: (1) the total cost of collection in  $\$/m^2$  ( $\$/ft^2$ ), (2) the reciprocal of the efficiency of the solar-to-thermal energy collection subsystem, and (3) the reciprocal of the applicable insolation in units of  $1/GJ/m^2\text{-sec}$  ( $1/M\text{ Btu}/ft^2\text{-yr}$ ). These factors are readily available or can be estimated. For example, the solar thermal energy collection subsystem cost for a low-cost heliostat or dish subsystem installed in a southwest U.S. location can be estimated as follows:

$$\begin{aligned} \text{Solar thermal energy collection} &= \frac{\text{total collection cost } (\$/ft^2)}{\text{subsystem cost (in English units)} \left[ \text{insolation } \frac{M\text{ Btu}}{ft^2\text{-yr}} \right] \left[ \text{collection efficiency} \right]} \\ &= 15 / [(0.9)(0.6)] \\ &= 28 \text{ } \$/M\text{ Btu/yr} \end{aligned}$$

To account for other solar energy collection concepts, site locations, and optical-to-thermal efficiencies a range of solar thermal energy subsystem collection costs from \$208/kJ/sec (\$7/M Btu/yr) to \$1666/kJ/sec (\$56/M Btu/yr) was used.

In addition, the issue of solar collection cost as a function of collection temperature was separately addressed. A survey of the reported solar thermal literature was conducted and the results are shown in figure E4. It is seen that reported collection cost is generally independent of collection or receiver temperature over the temperature range 93° C (200° F) to 760° C (1400° F). Higher collection costs at lower temperatures below 93° C (200° F) are mainly due to the inefficiency of flat-plate collectors operating in this regime. Collection costs at temperatures above about 538° C (1000° F) are probably underestimated because of the relative immaturity of these designs.

### c. Hybrid Plant Integration Cost

This parameter, applicable only to solar/fossil hybrid powerplants, was utilized to account for the expected additional cost of interfacing solar and fossil powerplant components. It is expressed in terms of a capital investment cost in \$/kWe.

The integration cost is expected to vary with both energy conversion subsystem type; e.g., gas turbine, combined cycle, and steam Rankine, and solar collection subsystem type; e.g., trough, dish and heliostat. Discussions with prime-mover manufacturers, powerplant vendors, and architect-engineering firms have established the costs previously shown in table E2. These costs are intended to be first-order estimates. Firmer estimates can be established when preliminary designs of hybrid powerplants are undertaken. The cost estimates used vary over a range of \$10/kWe for low capital cost powerplants to \$140/kWe for high capital cost plants. These correspond to 7 percent to 23 percent of the cost of the energy conversion subsystem.

#### d. Energy Storage Cost

The energy storage cost parameter is applicable to solar powerplants that utilize energy storage to extend electrical generation capacity beyond the available sun hours. Two values of this parameter, \$8.3/MWe sec (\$30/kWe hr) and \$27.8/MWe sec (\$100/kWe hr), were used. These were chosen to represent a realistic cost range for concepts applicable to solar thermal systems. A brief survey of the literature was conducted to estimate current capital costs of potential storage systems including thermal and nonthermal concepts. The results of that survey are shown in table E3. Most storage systems of interest are within the selected range. However, more recent studies (refs. 11 and 12) indicate that thermal storage in oil and pressurized water systems may yield cost below the specified range.

In addition, the retrieval efficiency of all storage systems was assumed to be 70 percent for this analysis.

#### e. Fixed Charge Rate

The fixed charge rate was treated as a parameter to evaluate the sensitivity of powerplant costs to possible future variations.

A nominal value of  $5.71 \text{ G sec}^{-1}$  ( $0.18 \text{ yr}^{-1}$ ) was assumed with variations of  $4.44 \text{ G sec}^{-1}$  ( $0.14 \text{ yr}^{-1}$ ) and  $6.97 \text{ G sec}^{-1}$  ( $0.22 \text{ yr}^{-1}$ ). The nominal value is that currently utilized by the utility industry. A breakdown of the nominal rate is shown in table E4.

#### f. Cost of Fuel

The cost of fuel parameter, expressed in \$/GJ (\$/M Btu), is applicable to both conventional and hybrid powerplants. Variation of this parameter ranged from \$0.47/GJ (\$0.50/M Btu) to \$3.80/GJ (\$4.00/M Btu) in 1975 dollars. These values represent current estimates of nuclear fuel and an upper bound of future oil or synthetic clean fuel costs, respectively. Intermediate values of \$0.95/GJ (\$1.00/M Btu) and \$2.37/GJ (\$2.50/M Btu) represent costs for coal and distillate fuel oil, respectively.

## g. Cost of Electricity

Five equations were formulated to calculate the relative (excludes operation and maintenance costs) busbar cost of electricity in mills/kWe hr for the four basic powerplant types considered. The additional equation was required to calculate the cost of solar energy collection per kilowatt of powerplant output from the solar energy collection subsystem cost.

The computer notation used in the equations is shown in table E5. An additional variable, HRS, the annual average operational kilowatt hours per day for a normalized plant generating capacity of 1 kWe is indicated. This variable is related to the plant capacity factor by the equation:

$$\text{Plant capacity factor} = (\text{HRS}/24)$$

Conventional powerplants: The cost of electricity of conventional powerplants (COEF) using fossil or nuclear fuel is given by:

$$\text{COEF} = \frac{(\text{COP})(\text{FCR})(24)(10^3)}{(\text{HRS})(8760)} + \frac{(\text{COF})(3413)(10^3)}{(10^6)(\text{EFF})}$$

The first term represents the powerplant capital cost contribution to cost of electricity, and the second term represents the fuel cost contribution to cost of electricity.

Solar standalone powerplant: The cost of electricity for solar standalone powerplants (COES) is given by:

$$\text{COES} = \frac{(\text{COC} + \text{COP})(\text{FCR})(10^3)(24)}{(\text{HRS})(8760)}$$

where  $\text{HRS} \leq 7$  for solar plant output and

$$\text{COC} = \frac{(\text{COCT})(3413)(8760)}{10^6 (\text{EFF})} \left( \frac{7}{24} \right)$$



Solar with storage powerplant: The equation for cost of electricity of solar with thermal storage powerplants (COESS) is given by:

$$\text{COESS} = \frac{(\text{COP} + \text{COC})(\text{FCR})(10^3)(24)}{(\text{HRS})(8760)} + \left[ \frac{\text{COC}}{(\text{EFFS})(7)} + \text{COS} \right] \left[ \frac{(\text{FCR})(10^3)(24)(\text{HRS} - 7)}{(\text{HRS})(8760)} \right]$$

where  $\text{HRS} \geq 7$  for thermal storage beyond solar plant output, and EFFS is 0.7 for this study.

Solar/fossil hybrid powerplant: The equation for cost of electricity of solar/fossil hybrid powerplants (COEH) is given by:

$$\text{COEH} = \frac{(\text{COP} + \text{COC} + \text{COI})(\text{FCR})(10^3)(24)}{(\text{HRS})(8760)} + \left( \frac{\text{COF}}{10^6} \right) \left[ \frac{(10^3)(3413)(\text{HRS} - 7)}{(\text{EFF})(\text{HRS})} \right]$$

where  $\text{HRS} \geq 7$  for fuel use beyond solar plant output time.

TABLE E1. - ECONOMIC ANALYSIS OPERATIONAL GROUND RULES

- All plants normalized to 1 kWe output power (maximum)
- Conventional plants can generate 24 kWe hr per day
- Hybrid plants can generate 24 kWe hr per day
- Non-hybrid solar standalone plants can generate 7 kWe hr on the average day
- Non-hybrid solar plus storage plants can generate 7 kWe hr per day plus storage capacity on the average day
- Energy storage subsystems can provide 1 kWe output power for up to operational storage time (capacity)

TABLE E2. - SELECTED VALUES OF PARAMETERS

Parameter	Value	
Energy Conversion Subsystem	\$/kWe	
Gas turbine	150	
Combined cycle	300	
Steam Rankine	600	
Nuclear	800	
Fuels for Energy Conversion Subsystem	\$/GJ	\$/M Btu
Nuclear	0.47	0.50
Coal	0.95	1.00
Oil	2.37	2.50
Future oil or advanced synthetic	3.80	4.00
Solar Thermal Energy Collection Subsystem	\$/kJ/sec	\$/M Btu/yr
Low cost flat plate	208	7
Low cost trough, flat plate	416	14
Low cost heliostat/dish, trough	833	28
Heliostat/dish	1666	56
Hybrid Plant Integration Cost	\$/kWe	
Low estimate (for gas turbines)	10	
Intermediate (for combined cycle/steam Rankine)	70	
High (for steam Rankine)	140	
Energy Storage Subsystem	\$/MWe sec	\$/KWe hr
Estimated range of values for 6 hr capacity	8.3, 27.8	30, 100
Annual Fixed Charge Rate	G sec <sup>-1</sup>	Yr <sup>-1</sup>
Low estimate	4.44	0.14
Nominal value	5.71	0.18
High estimation	6.97	0.22

ORIGINAL PAGE IS  
OF POOR QUALITY

TABLE E3. - ENERGY STORAGE

COST ESTIMATES<sup>a</sup>

Type	Cost \$/MWe sec (\$/kWe hr)
<b>Thermal</b>	
Caloria-rock	22 (80)
Sodium hydroxide	11 (40)
Steel ingot	14 (50)
Caloria-Hitec	41.7 (150)
Eutectic salt	24 (85)
Therminol 66	44 (160)
<b>Nonthermal</b>	
Pumped hydro	8.3 (30)
Compressed air	8.3 (30)
Redox battery	11 (40)
Lead-acid battery	17 (60)
Chemical	17 (60)
Flywheel	27.8 (100)

<sup>a</sup>6 hr storage.

TABLE E4. - FIXED CHARGE

## RATE BREAKDOWN

Item	Rate $G \text{ sec}^{-1}$ ( $\text{yr}^{-1}$ )
Cost of money	2.378 (0.075)
Federal income tax	1.300 (0.041)
Depreciation	1.046 (0.033)
Other taxes	0.888 (0.028)
Insurance	0.032 (0.001)
Working capital	0.063 (0.002)
	<u>5.71 (0.180)</u>

TABLE E5. - VARIABLE NOTATION

Variable	Computer notation	English units
Solar thermal energy collection subsystem cost	COCT	\$/M Btu/yr
Solar energy collection subsystem cost	COC	\$/kWe
Energy conversion subsystem cost	COP	\$/kWe
Energy conversion efficiency	EFF	percent
Fixed charge rate	FCR	$\text{yr}^{-1}$
Fuel cost	COF	\$/M Btu
Energy storage cost	COS	\$/kWe hr
Energy storage efficiency	EFFS	percent
Hybrid plant integration cost	COI	\$/kWe
Annual average operational time	HRS	hr/day

## REFERENCES

1. Wolfe, R. W.; et. al.: Energy Conversion Alternatives Study (ECAS), vol. XI, Advanced Steam Systems. (76-9E9-ECAS-Rlv-11, Westinghouse Electric Corp.; NASA Contract NAS3-19407.) NASA CR-134941, 1976.
2. Todd, D. M.: Design and Application of Heat Recovery Steam Generators. GER 2478 General Electric Company, 1970.
3. Gupta, B. P.; et. al.: Technical Feasibility Study of Modular Disk Solar Electric Systems. (ERDA/NASA-19740/76/1, Honeywell, Inc.; Black and Veatch Consulting Engineers; NASA Contract NAS3-19740.) NASA CR-135012, 1976.
4. Wilson, W. B.; and Kovcik, J. M.: Gas Turbine Energy Systems for the Process Industries. GER 2229H, General Electric Company, 1966.
5. Solar-Thermal Conversion to Electricity Utilizing a Central-Receiver, Open-Cycle Gas Turbine Design. ER-387-SY, Electric Power Research Inst., 1976.
6. Brown, D. H.; and Corman, J. C.: Energy Conversion Alternatives Study (ECAS), vol. II, Advanced Energy Conversion Systems, Part 1, Open Cycle Gas Turbines. (SRD-76-011, General Electric Company, NASA Contract NAS3-19406.) NASA CR-134948, 1976.
7. DOT/NASA Comparative Assessment of Brayton Engines for Guideway Vehicles and Buses, vol. II - Analysis and Results. NASA SP-354, 1975.
8. Zoschak, R. J.; and Wu, S. F.: Studies of the Direct Input of Solar Energy to a Fossil-Fueled Central Station Steam Powerplant. Sol. Energy, vol. 17, no. 5, 1975, pp. 297-305.
9. Technical and Economic Feasibility of Solar Augmentation for Boiler Feedwater Heating in Steam-Electric Power Plants. F-C4362, Franklin Institute Research Laboratories, 1976. (See also COO-2864-1, ERDA.)

10. Albertson, V. D.: Solar Hybrid Plants: Power System Interface Analysis. COO-2699-2, ERDA, 1975.
11. Dooley, James L., et. al.: A Feasibility Study of Underground Energy Storage Using High-Pressure, High-Temperature Water. RDA-TR-7100-001, R&D Associates, 1977. (See also CONS/1243-1, ERDA.)
12. Retrofitted Feedwater Heat Storage for Steam Electric Power Stations Peaking Power Engineering Study. Final Report, Bechtel Corp., 1976. (See also CONS/2863-1, ERDA.)

TABLE I. - SELECTED ENERGY CONVERSION SUBSYSTEMS

Gas Cycles

1. Simple open Brayton cycle gas turbine
2. Recuperated open Brayton cycle gas turbine

Vapor Cycles

1. Regenerative (feedwater heated) Rankine cycle superheated steam turbine

Combined Cycles

1. Simple and recuperated open Brayton cycle gas turbine and unfired Rankine cycle superheated steam turbine
2. Simple open Brayton cycle gas turbine and supplementary fired Rankine cycle superheated steam turbine

TABLE II. - PEAK OPERATING TEMPERATURE OF  
STEAM RANKINE CYCLE,  $T_g$ , °C (°F)

$T_5$ , $\epsilon$	982° C (1800° F)	1038° C (1900° F)	1093° C (2000° F)	1204° C (2200° F)	$T_g$
0	453 (847)	473 (884)	494 (922)	539 (1003)	
.3	417 (782)	439 (822)	462 (863)	508 (947)	
.5	374 (705)	395 (743)	417 (782)	460 (860)	
.7	310 (590)	328 (623)	346 (655)	382 (720)	
.8	263 (505)	279 (534)	294 (562)	325 (617)	

Note: Steam temperatures correspond to maximum thermal efficiency of combined gas turbine cycle.



TABLE III. - TYPICAL BREAKDOWN OF THERMAL ENERGY REQUIREMENTS FOR  
TWO STEAM RANKINE CYCLE POWERPLANTS

Thermal energy input station	Temperature range, °C (°F)	Thermal energy input - percent	
		8.3 MN/m <sup>2</sup> (1200 psi) steam plant	16.6 MN/m <sup>2</sup> (2400 psi) steam plant
Feedwater heaters	38-260 (100-500)	24.8	25.4
Economizer (preheater)	260-371 (500-700)	8.0	19.4
Evaporator (boiler)	316-371 (600-700)	35.5	18.5
Superheater	316-538 (600-1000)	19.8	24.4
(Evaporator plus superheater)	316-538 (600-1000)	(55.3)	(42.9)
Reheater	316-538 (600-1000)	11.9	12.3
Total		100.0	100.0

TABLE IV. - COST INPUT PARAMETERS FOR ECONOMIC COMPARISON

Powerplant Type	Case	Solar thermal energy collection cost, \$/MJ/sec, (\$/M Btu/yr)	Energy conversion (plant) cost, \$/kWe	Hybrid plant integration cost, \$/kWe	Energy storage cost, \$/MWe sec, (\$/kWe hr)	Fossil fuel cost, \$/GJ (\$/M Btu)	Energy conversion thermal efficiency, percent
Advanced hybrid-recuperated gas turbine cycle	A	.83 (28)	150	10	-----	2.37 (2.50)	50
Retrofit hybrid-simple gas turbine cycle	B	.83 (28)	150	10	-----	2.37 (2.50)	34
Retrofit hybrid-steam Rankine cycle	C	.83 (28)	600	70	-----	2.37 (2.50)	40
Solar thermal steam Rankine cycle Low cost energy storage	D	.83 (28)	600		8.3 (30)	-----	40
High cost energy storage	E	.83 (28)	600		27.8 (100)	-----	40

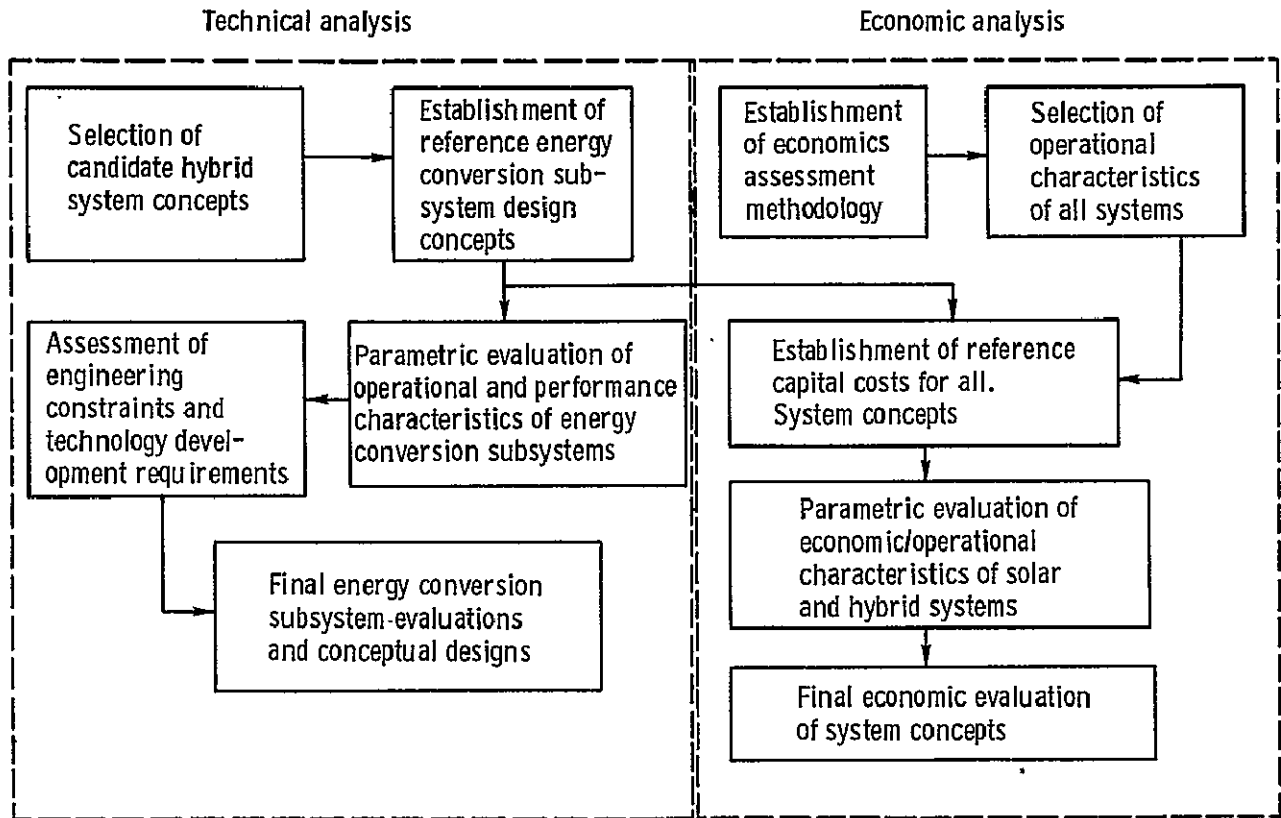


Figure 1. - Study methodology flow diagram.

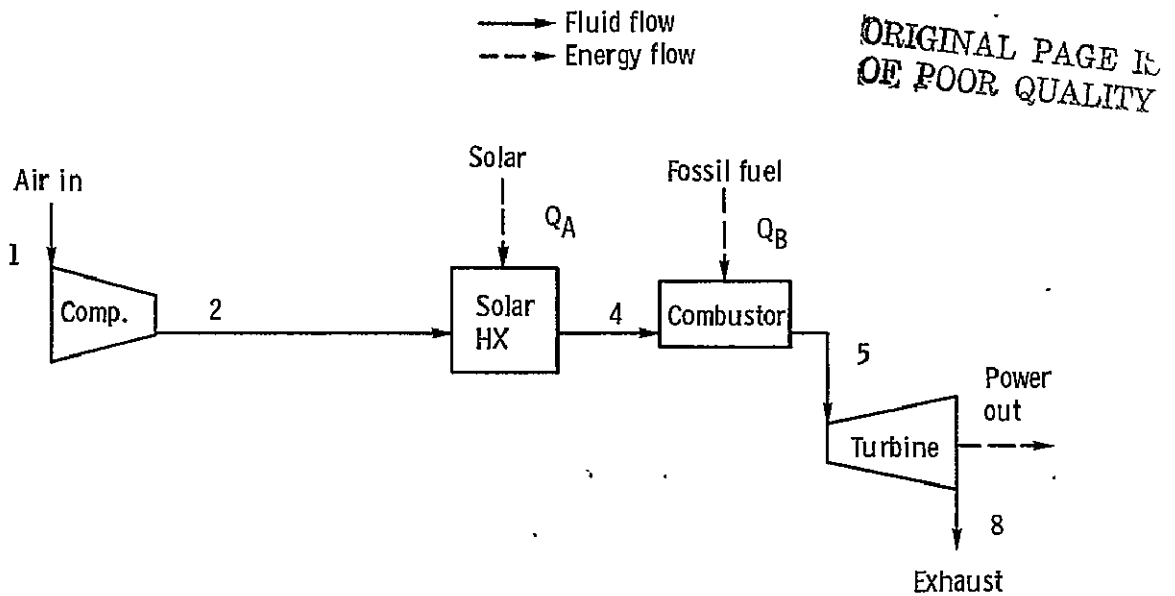


Figure 2. - Diagram of simple gas turbine cycle. Hybrid system.

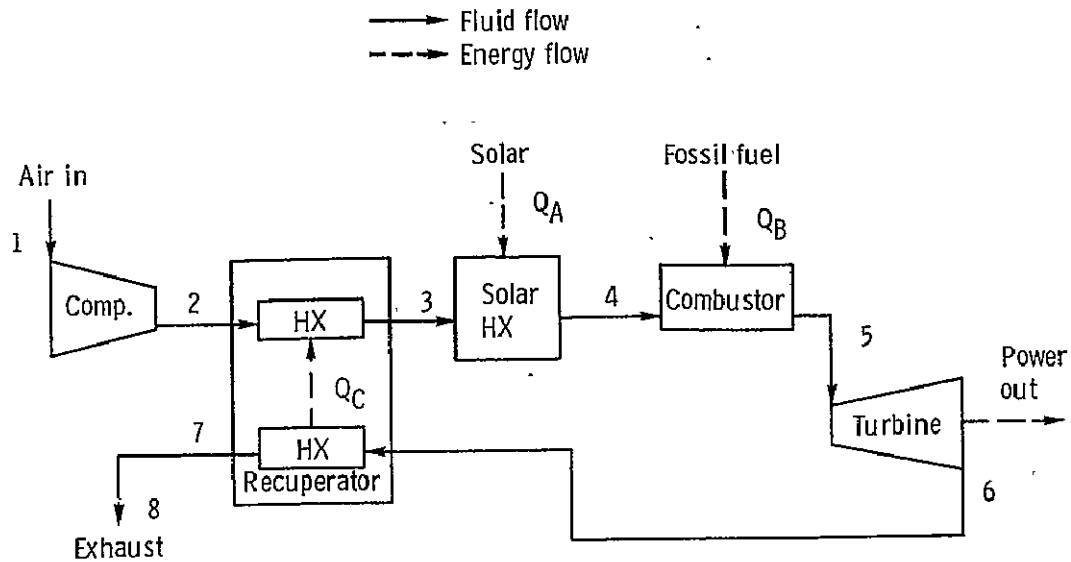


Figure 3. - Diagram of recuperated gas turbine cycle. Hybrid system.

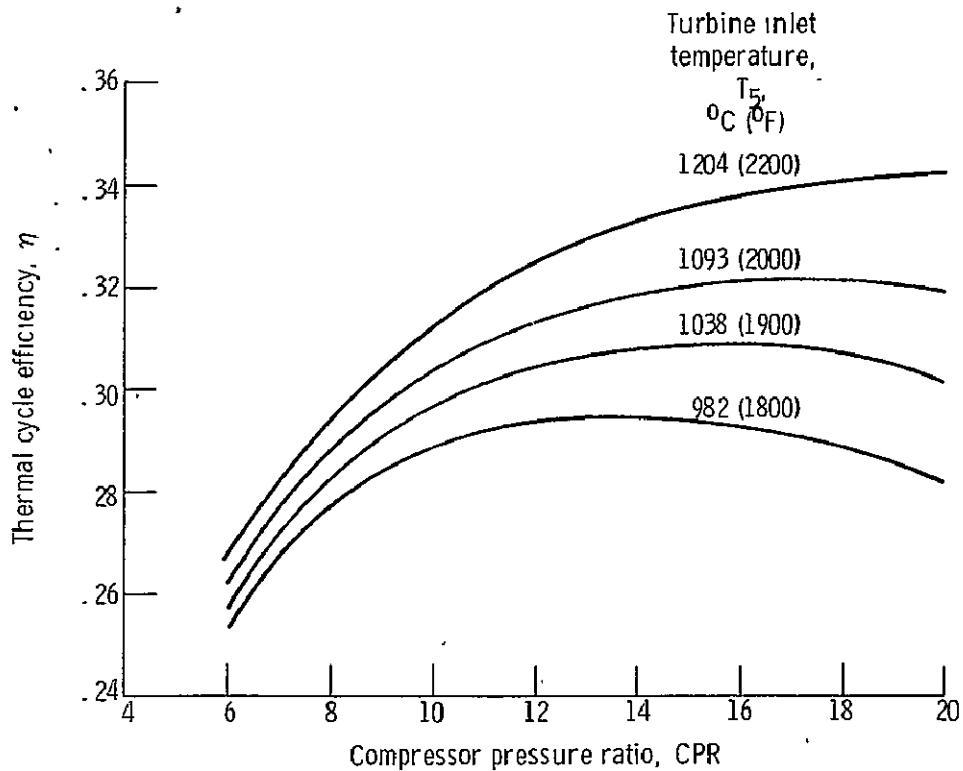


Figure 4. - Thermal cycle efficiency of simple gas turbine cycle.

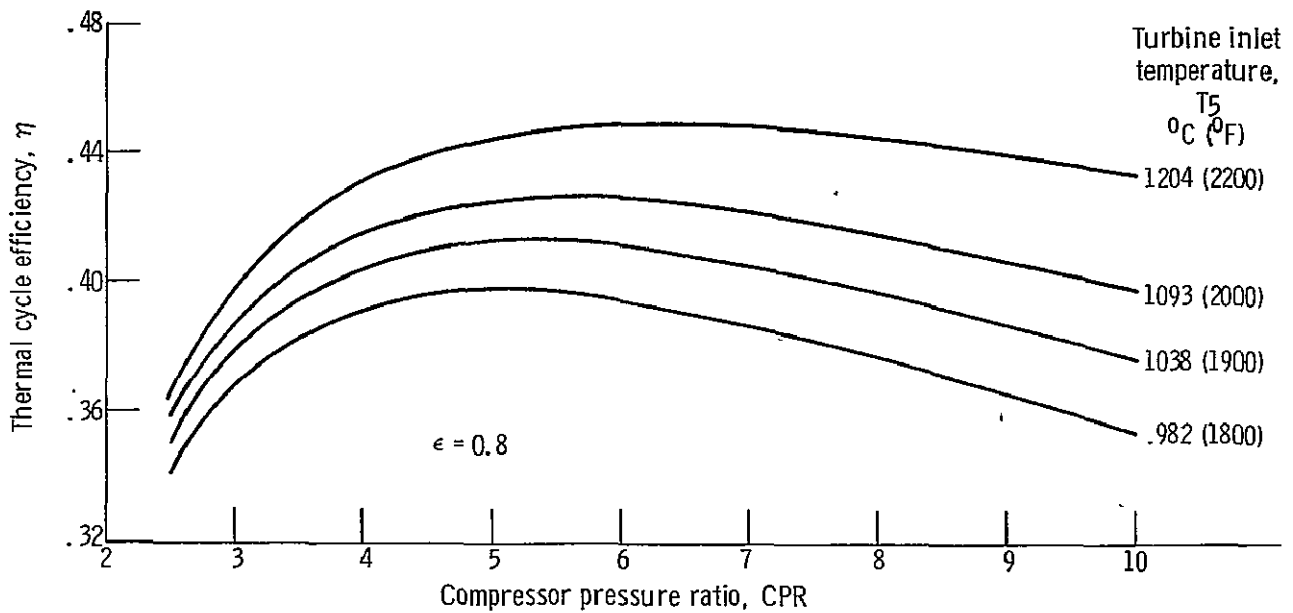


Figure 5. - Thermal cycle efficiency of a recuperated gas turbine cycle.

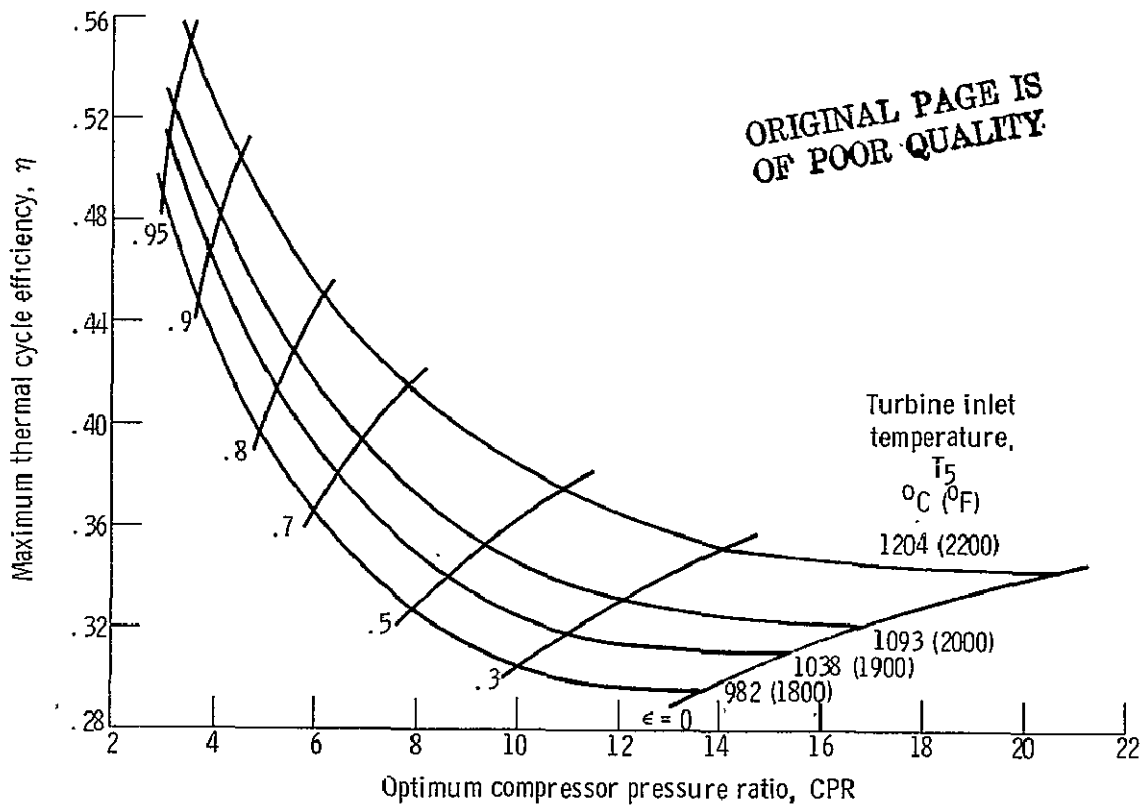


Figure 6. - Maximum thermal cycle efficiency of simple and recuperated gas turbine cycles.

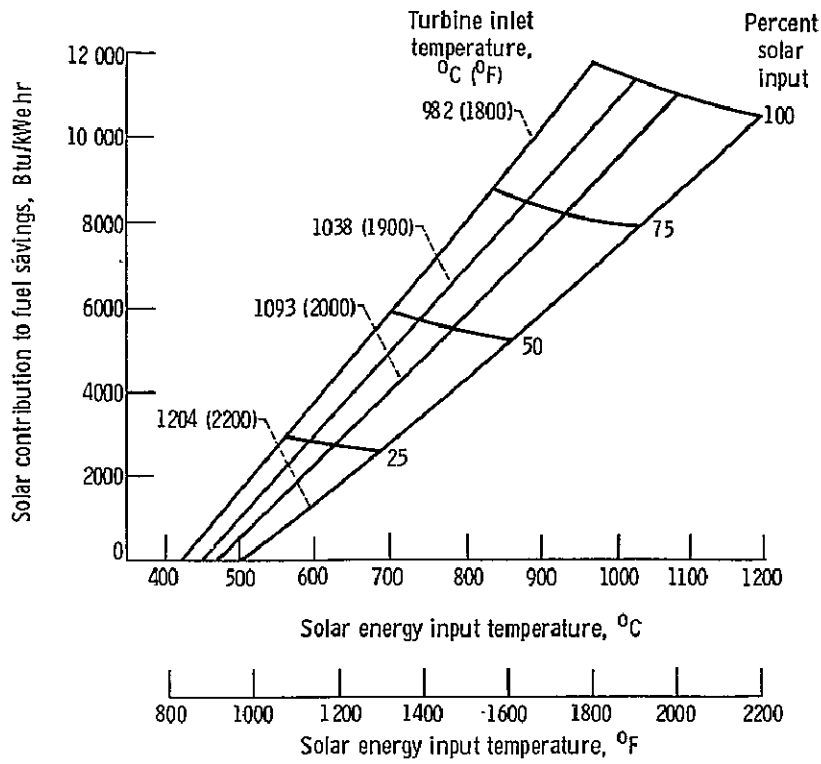


Figure 7. - Solar fuel savings for optimized simple gas turbine open cycle hybrids.

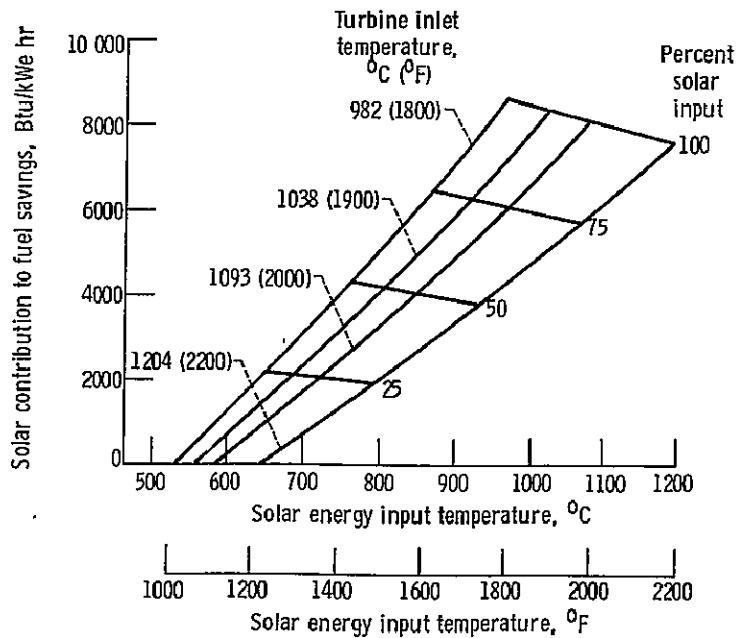


Figure 8. - Solar fuel savings for optimized recuperated gas turbine open cycle hybrids ( $\epsilon = 0.8$ ).

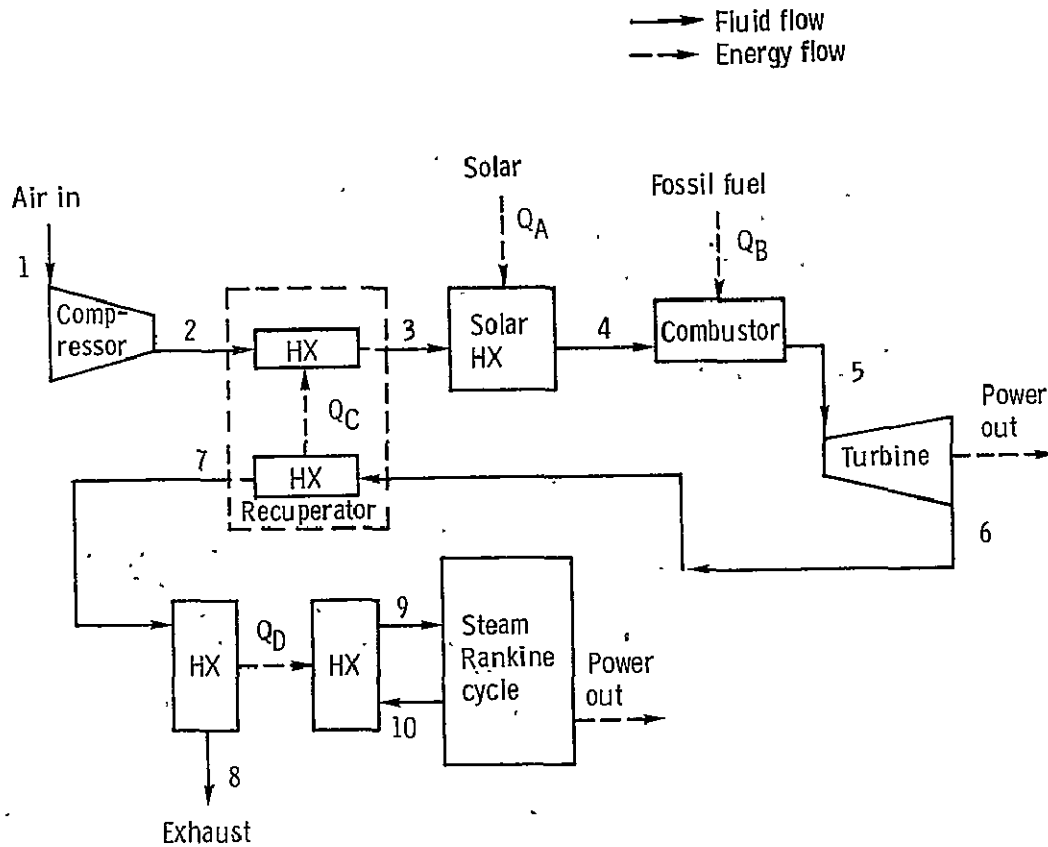


Figure 9. - Diagram of combined gas turbine-steam Rankine cycle hybrid system.

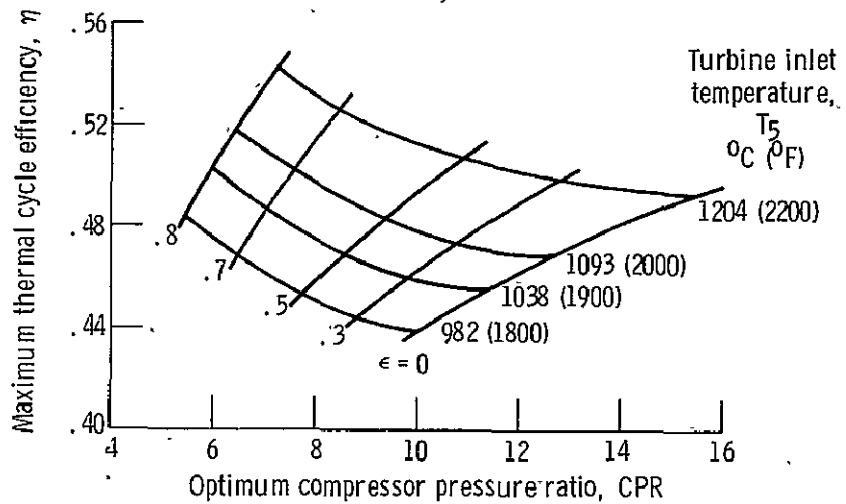


Figure 10. - Maximum thermal cycle efficiency of a combined cycle.

ORIGINAL PAGE IS  
OF POOR QUALITY

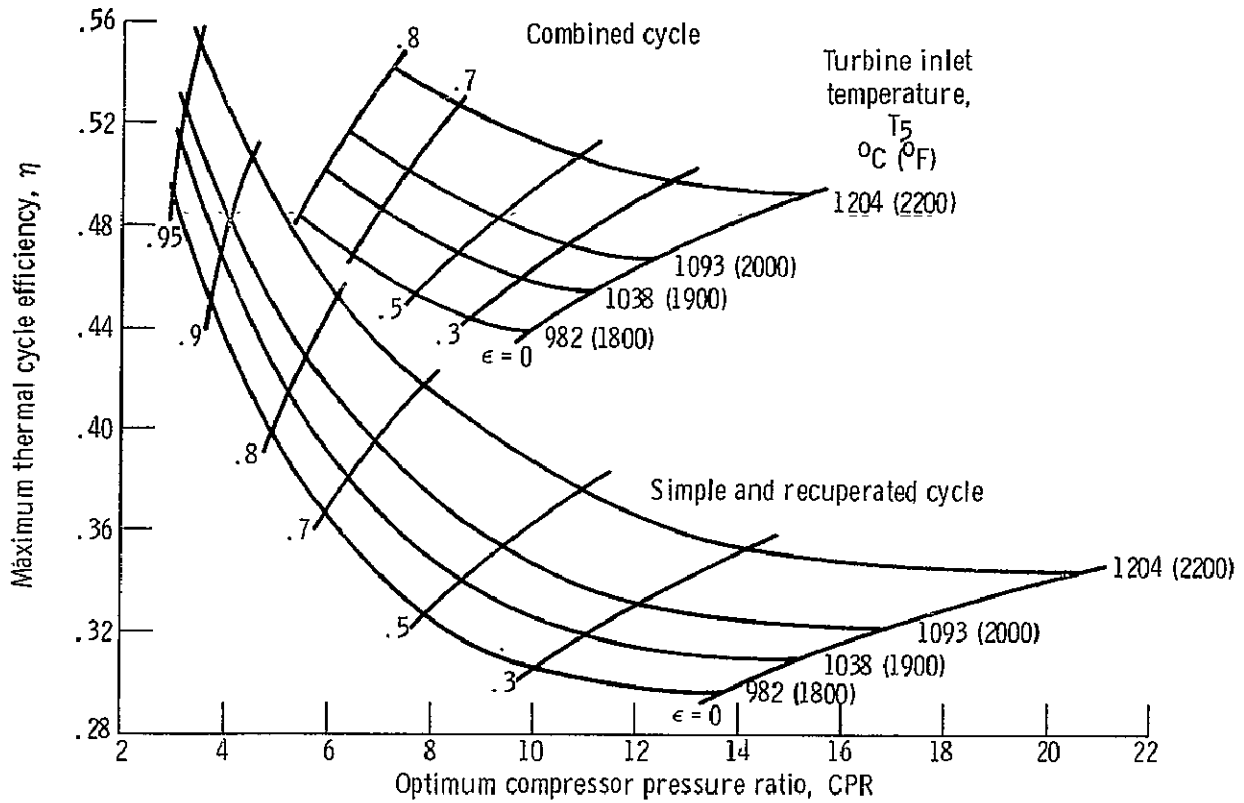


Figure 11. - Maximum thermal cycle efficiency of simple, recuperated, and combined gas turbine cycles.

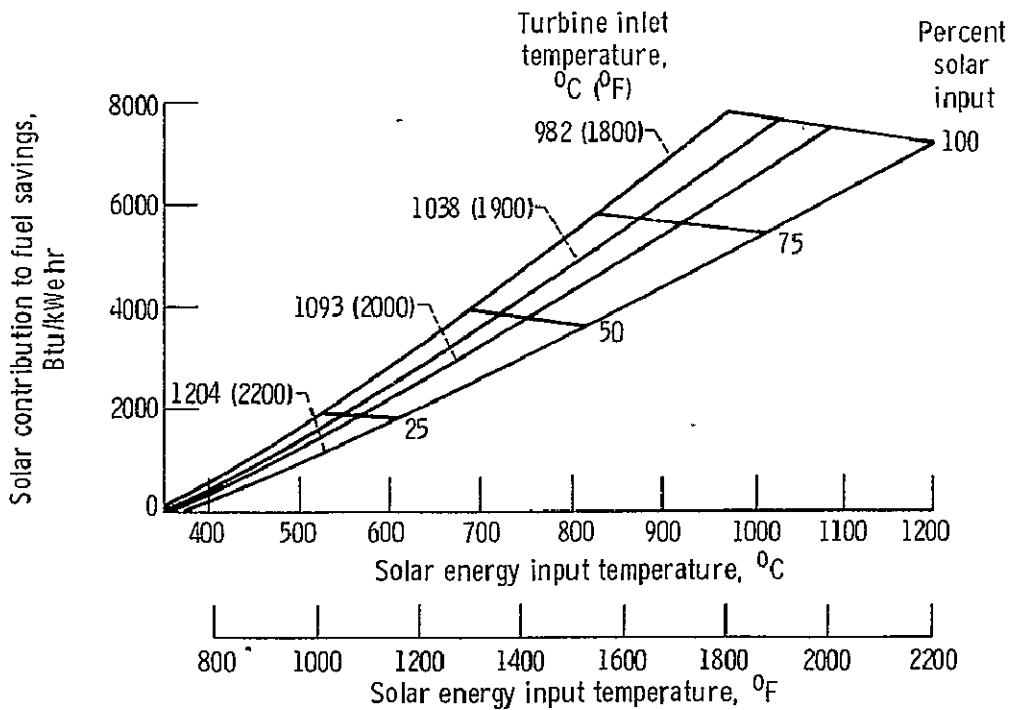


Figure 12. - Solar fuel savings for optimized simple combined cycle hybrids.



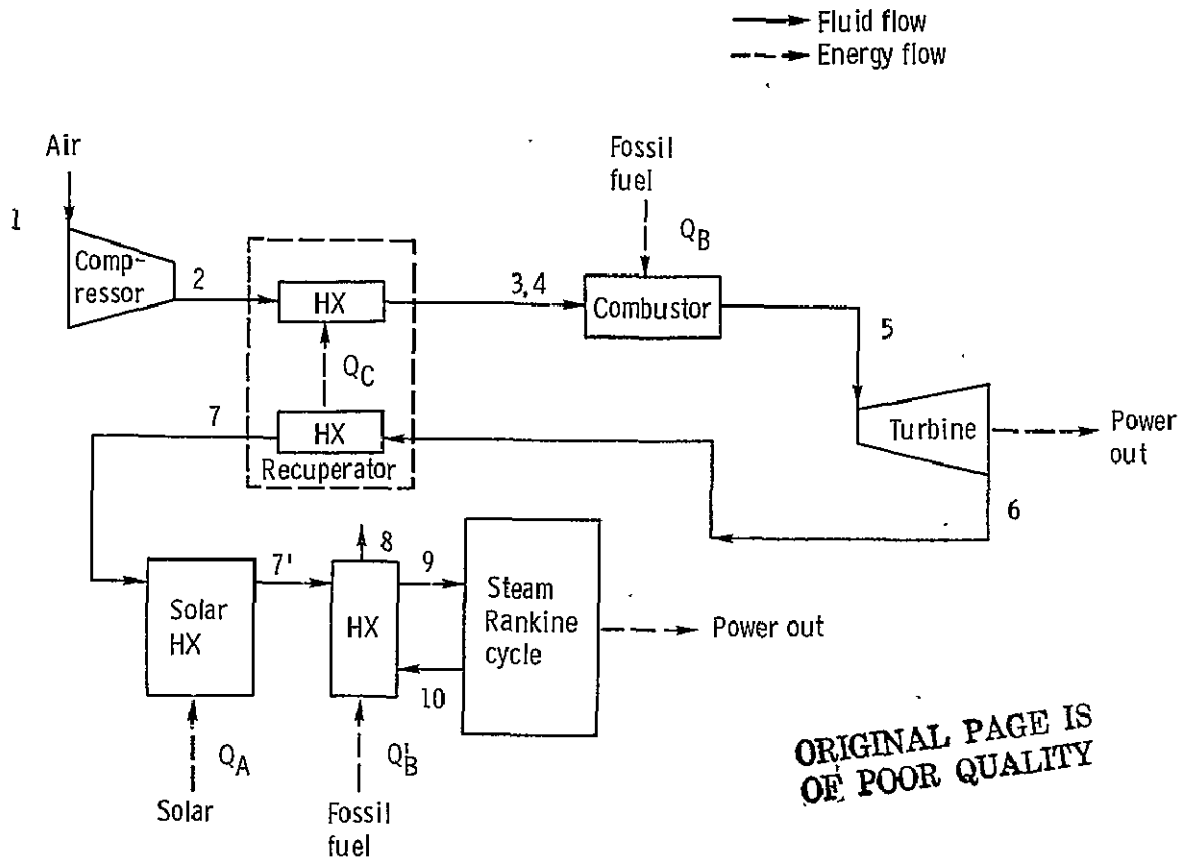


Figure 13. - Diagram of supplemental-fired combined cycle hybrid system.

**ORIGINAL PAGE IS  
OF POOR QUALITY**

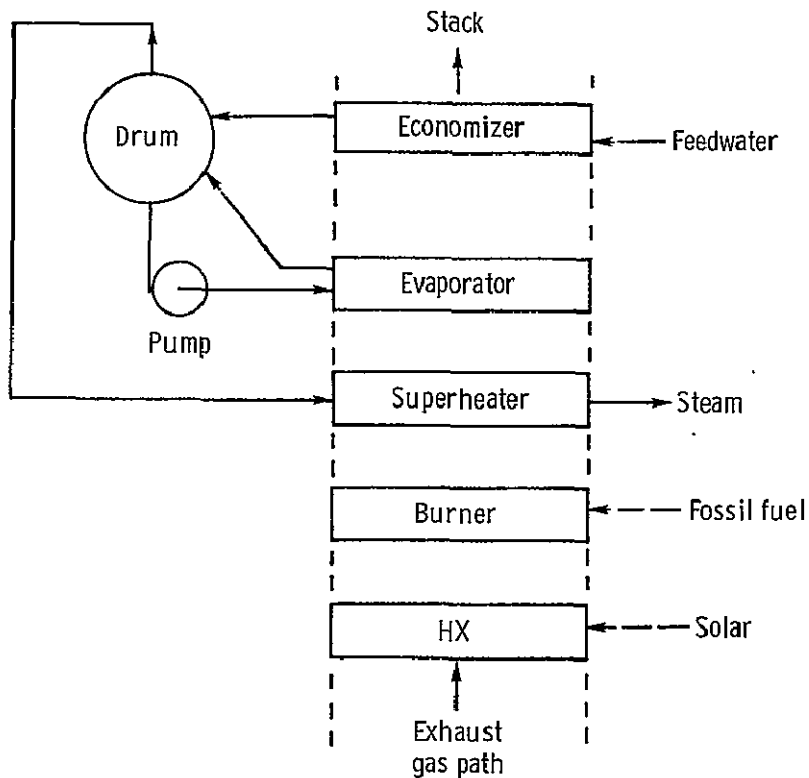


Figure 14. - Concept for configuration of supplemental-fired combined cycle hybrid system.

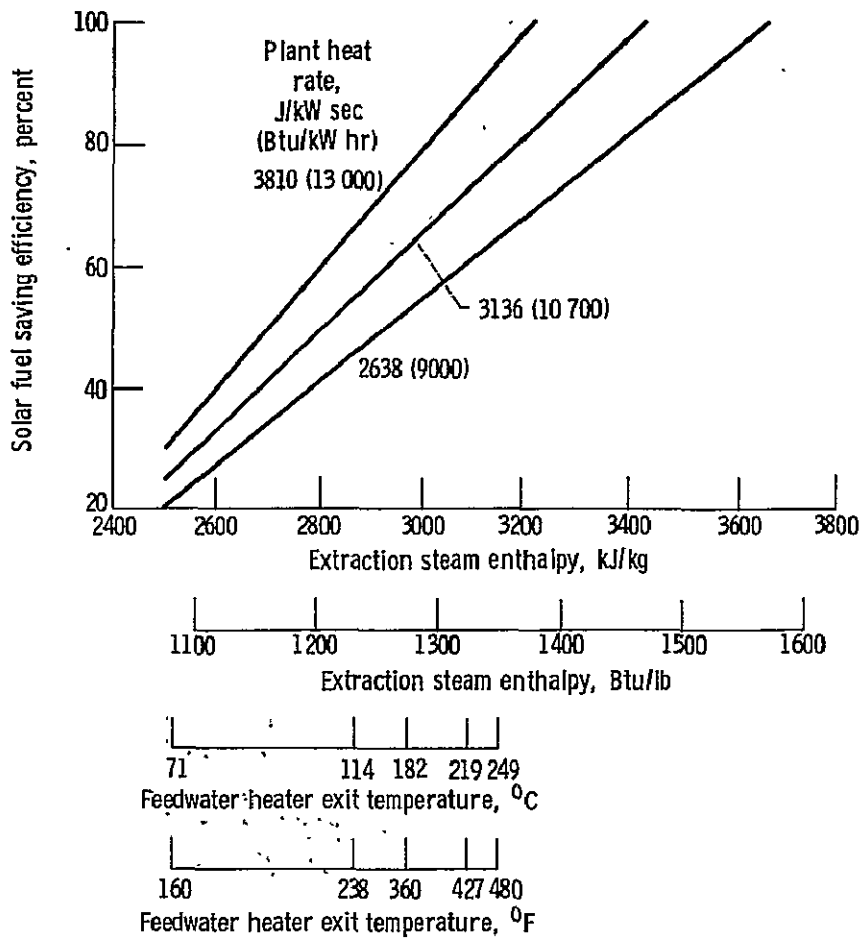


Figure 15. - Solar fuel savings efficiency of steam vapor cycle hybrid system (from ref. 9).

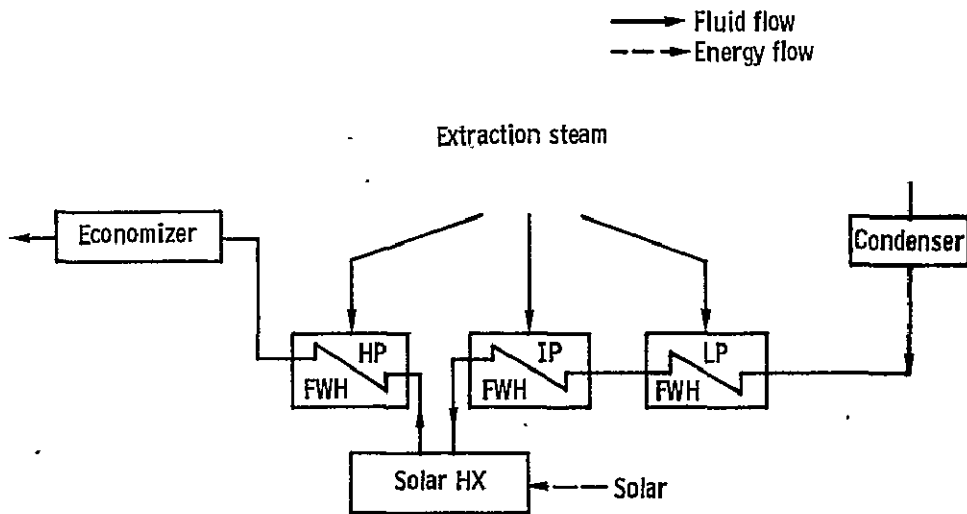


Figure 16. - Solar hybrid augmentation of feedwater heating (series configuration) for steam Rankine powerplant.

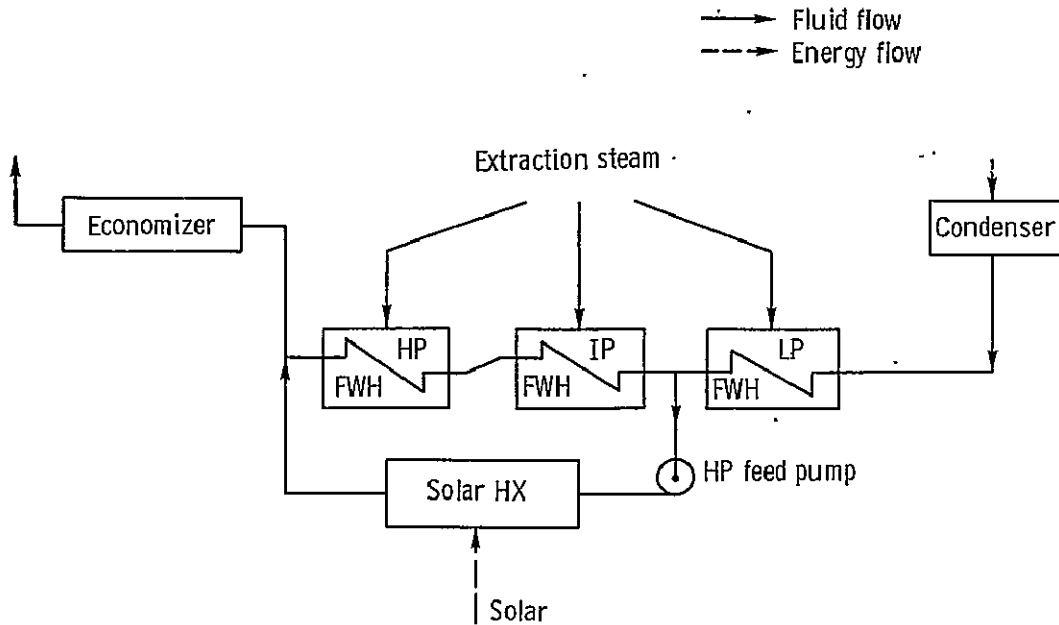


Figure 17. - Solar hybrid augmentation of feedwater heating (parallel configuration) for steam Rankine powerplant.

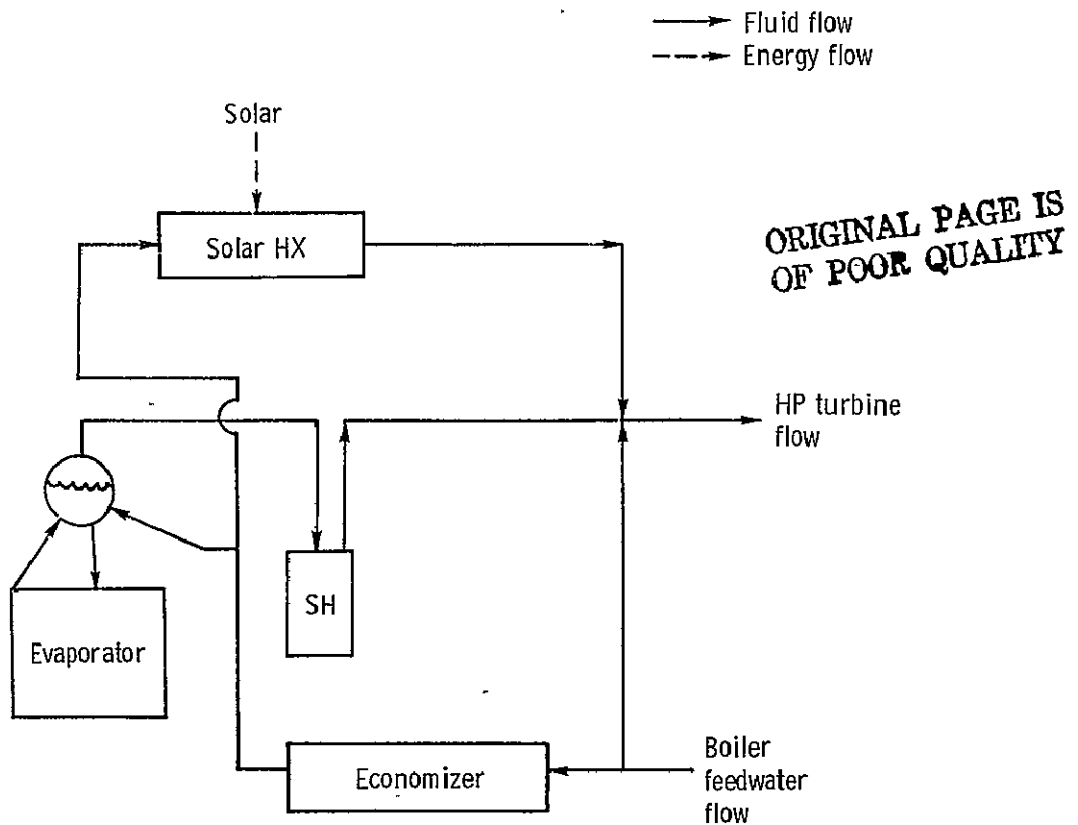


Figure 18. - Solar hybrid augmentation of combined evaporation and superheating (parallel configuration) for steam Rankine powerplant.

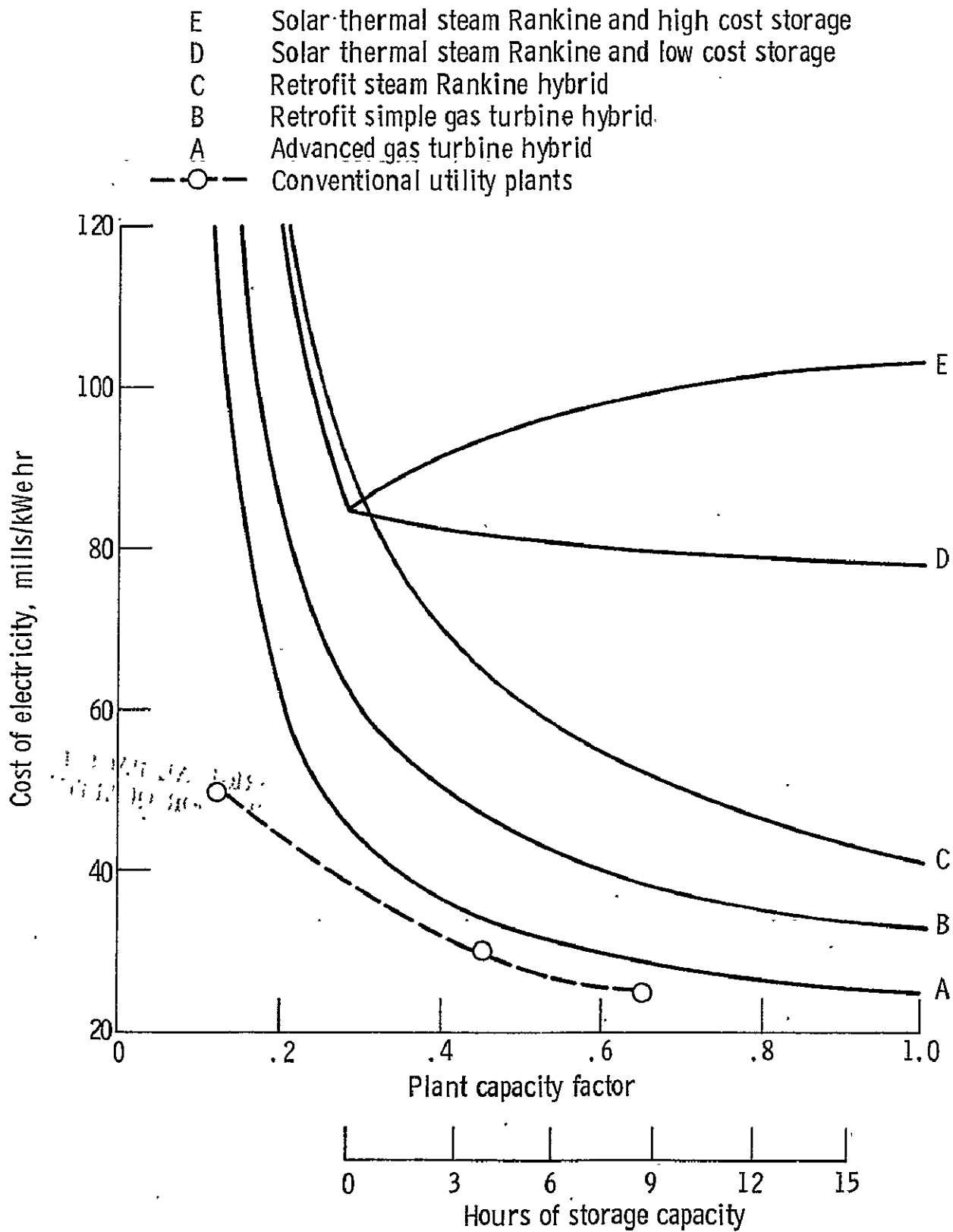


Figure 19. - Overall economic comparison of hybrid powerplant types using current estimates of solar collection costs.

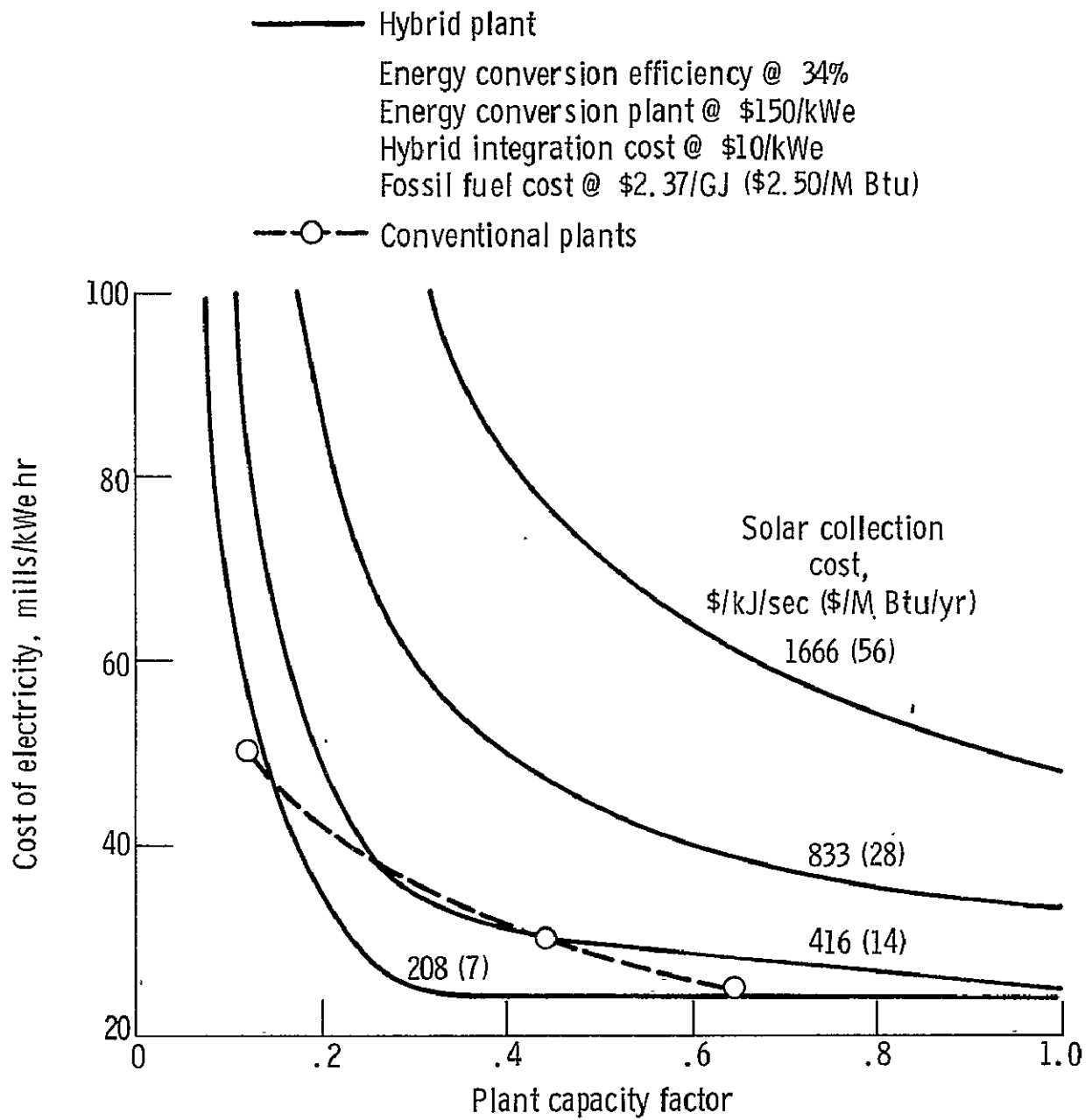


Figure 20. - Effect of solar energy collection cost on cost of electricity for a gas turbine hybrid powerplant.

ORIGINAL PAGE IS  
OF POOR QUALITY

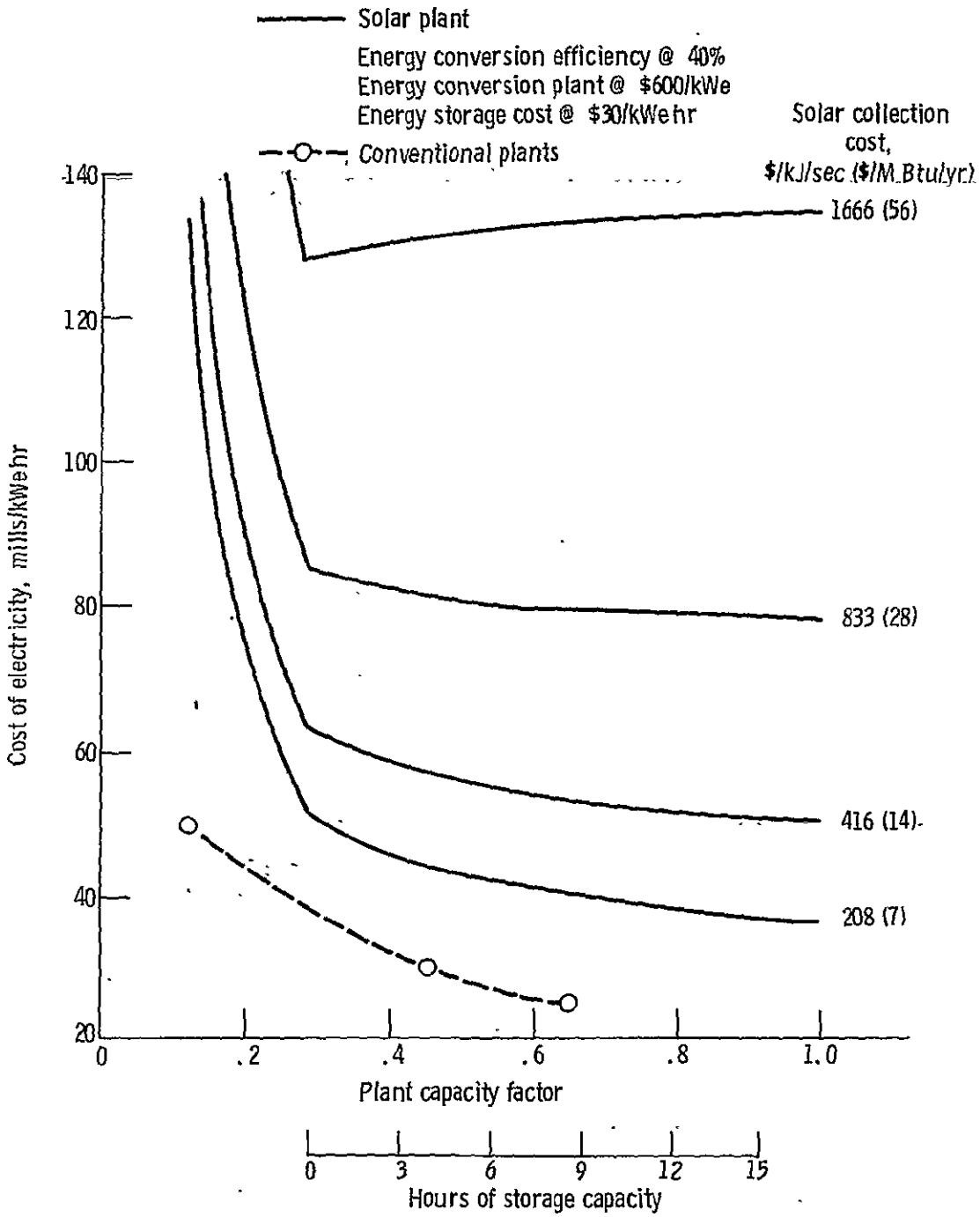


Figure 21. - Effect of solar energy collection cost on cost of electricity for a steam Rankine solar powerplant with thermal storage.

THE BUREAU OF RESEARCH  
 NATIONAL BUREAU OF STANDARDS  
 WASHINGTON, D. C. 20540

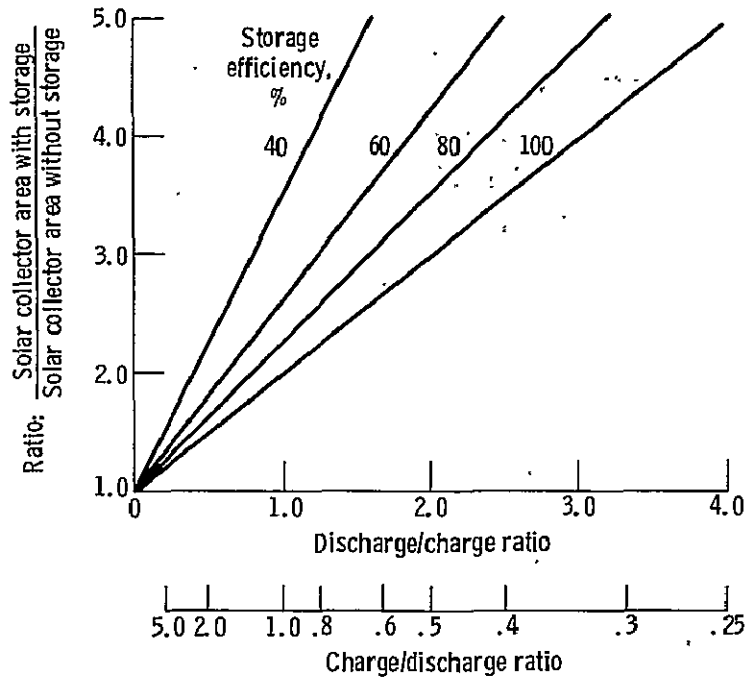
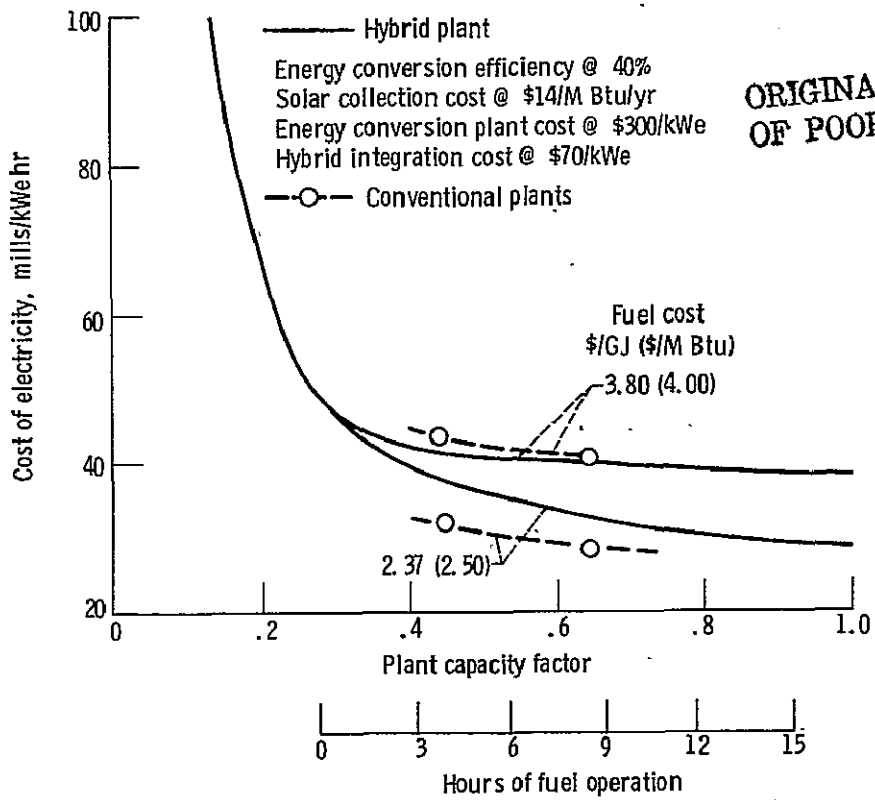


Figure 22. - Effect of storage subsystem on solar collection area.



ORIGINAL PAGE IS OF POOR QUALITY

Figure 23. - Effect of fuel cost on cost of electricity for combined cycle hybrid powerplants.

— Hybrid plants  
 Energy conversion efficiency @ 34%  
 Solar collection cost @ \$416/kJ/sec (\$14/M Btu/yr)  
 Fossil fuel cost @ \$2.37/GJ (\$2.50/MMBtu)

—○— Conventional plants

Curve	Hybrid integration cost (\$/kWe)
A, D	10
B, E	70
C, F	140

A, B, C Energy conversion cost (\$/kWe)  
 Gas turbine cycle @ 150  
 D, E, F Steam Rankine cycle @ 600

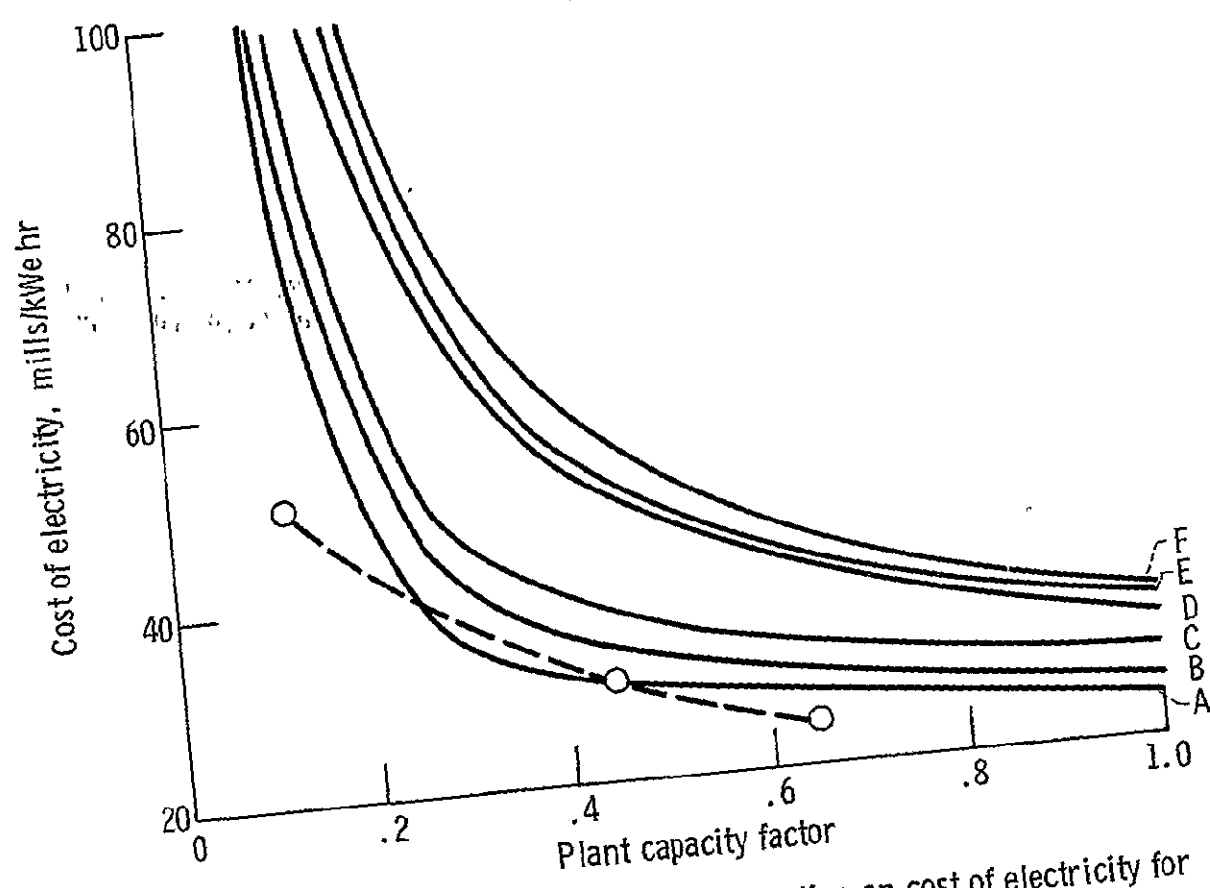


Figure 24. - Effect of hybrid cost of integration on cost of electricity for two hybrid retrofit powerplants.



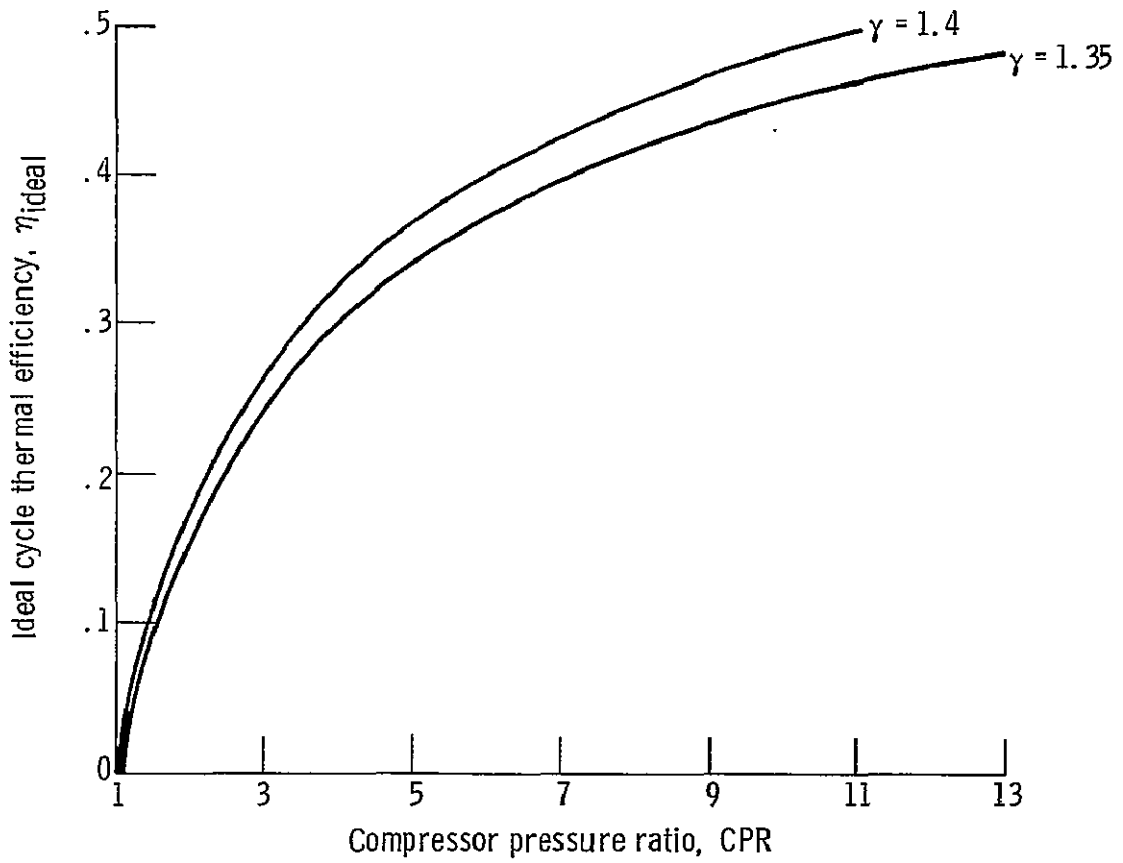


Figure D1. - Ideal thermal efficiency of simple gas turbine cycle.

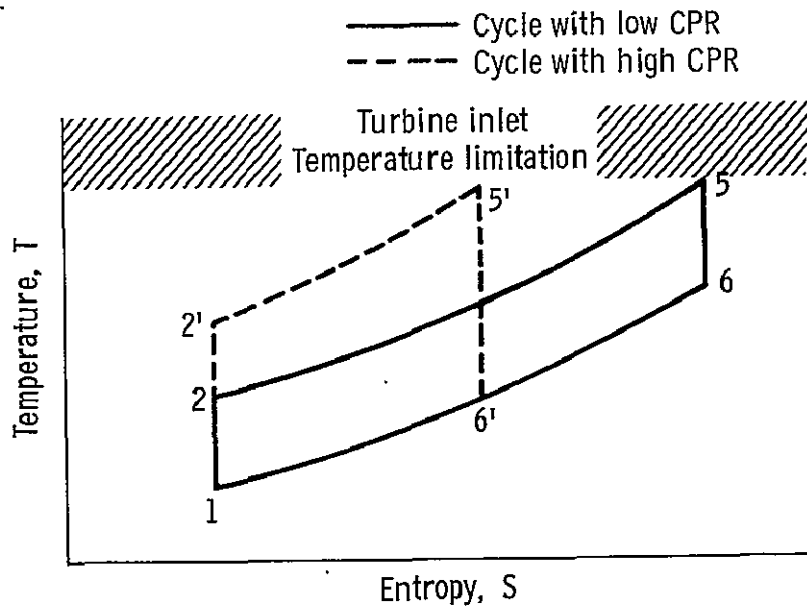


Figure D2. - T-S diagram of ideal simple gas turbine cycle.

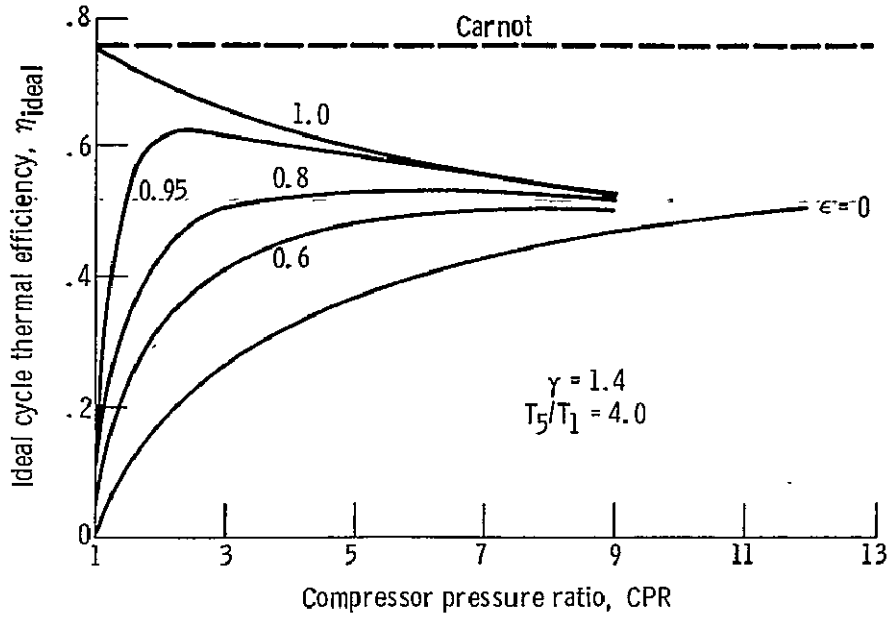


Figure D3. - Ideal thermal efficiency of simple and recuperated gas turbine cycles.

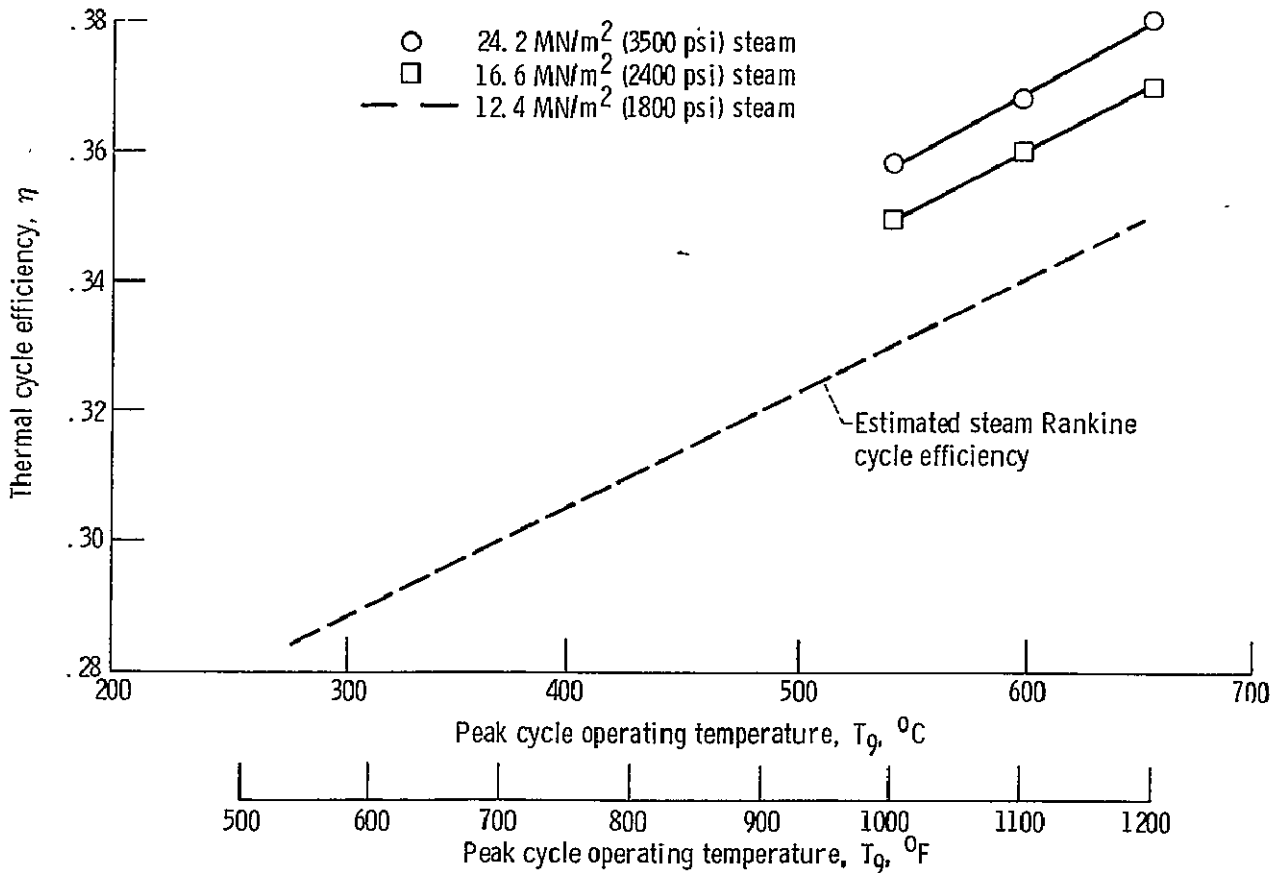


Figure D4. - Assumed variation of steam Rankine cycle efficiency.

ORIGINAL PAGE IS  
OF POOR QUALITY

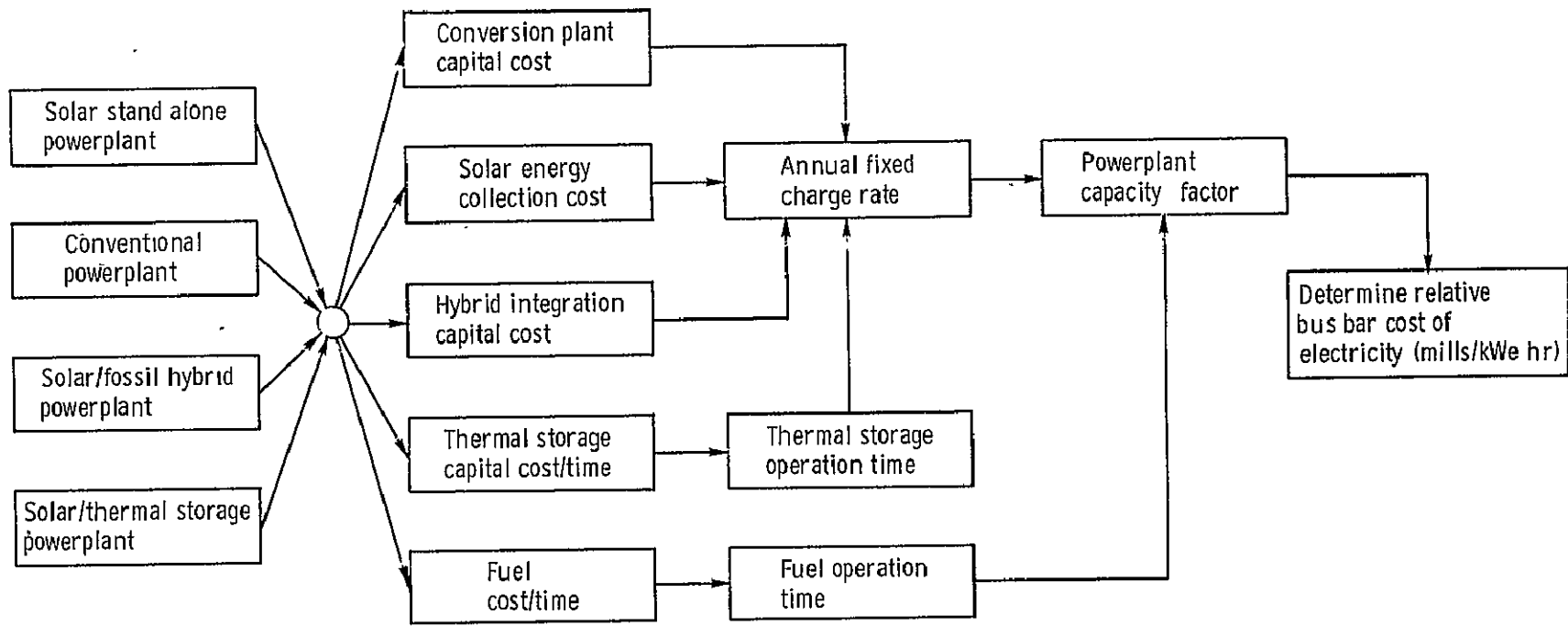


Figure E1. - Economic analysis methodology.

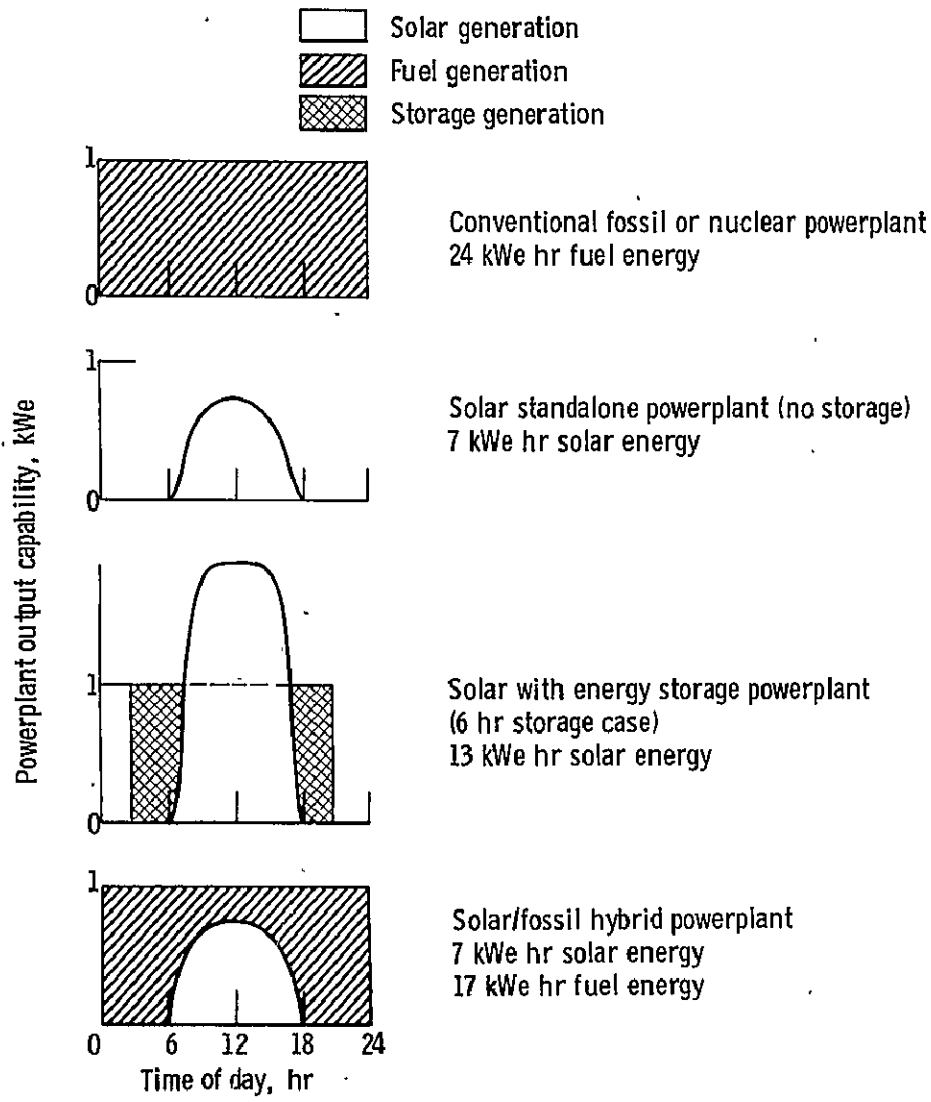


Figure E2. - Comparison of average day powerplant capabilities.

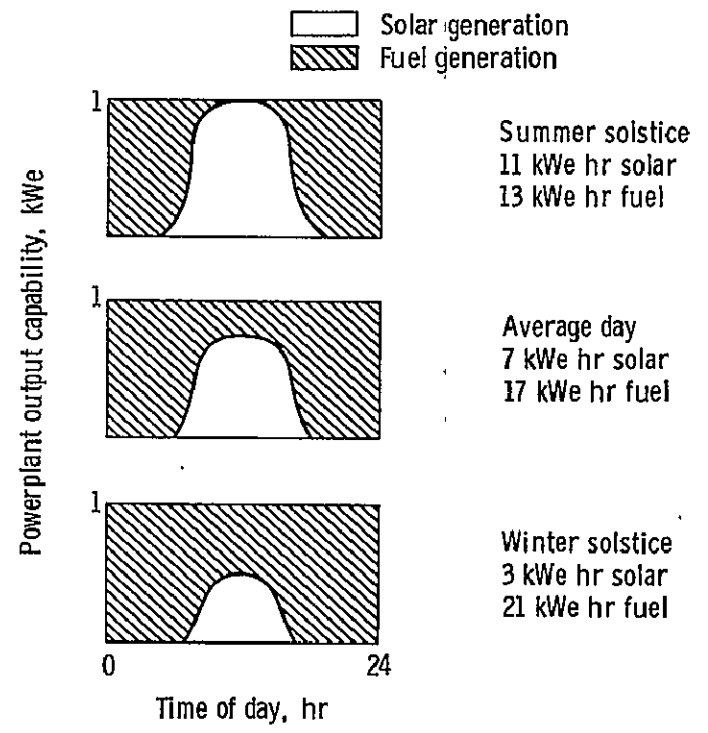


Figure E3. - Solar hybrid powerplant operational capability.

- ① Flat plate - air and water (PPG, Corning, Chamberlain, GE, ITC, OI)
- ② Parabolic trough - pressurized water (Honeywell, U of M, Sheldahl)
- ③ Parabolic dish - superheated steam (Honeywell, Itek)
- ④ Central receiver - superheated steam (Honeywell, MDAC, U of H, Sheldahl, M-M)
- ⑤ Parabolic dish - NaK (Honeywell)
- ⑥ Parabolic dish - chemical, gas (JPL)

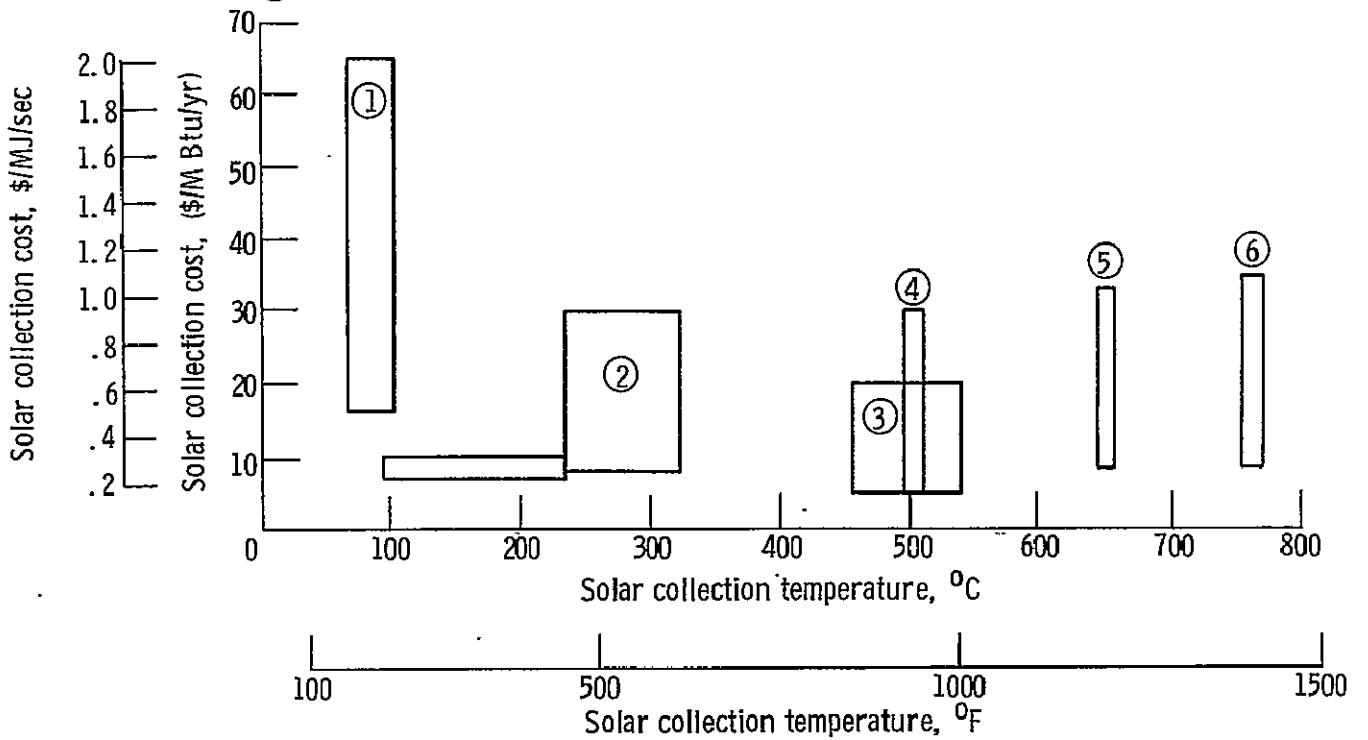


Figure E4. - Solar collection cost versus collection temperature.

ORIGINAL PAGE IS  
OF POOR QUALITY

NATIONAL AERONAUTICS AND SPACE ADMINISTRATION  
WASHINGTON, D.C. 20546

OFFICIAL BUSINESS  
PENALTY FOR PRIVATE USE \$300

SPECIAL FOURTH-CLASS RATE  
BOOK

POSTAGE AND FEES PAID  
NATIONAL AERONAUTICS AND  
SPACE ADMINISTRATION  
451



POSTMASTER : If Undeliverable (Section 158  
Postal Manual) Do Not Return

---